Expression, Purification and Characterization of the Biotin Transporter from *Staphylococcus aureus*

By

Weiwei Tang

B.Sc. (Biotechnology)

This thesis is submitted in part fulfillment of the requirement for the degree of Master Philosophy of Science in Biochemistry

Discipline of Biochemistry,

School of Molecular and Biomedical Science,

The University of Adelaide

Adelaide, South Australia, 5005

July 2013

TABLE OF CONTENTS

STATEMENT OF ORIGINALITY

This thesis contains no material that has been accepted for the award of any degree or diploma by any University and, to the best of my knowledge, contains no material that has been previously published by any other person, except where due reference has been made in the text.

This thesis is presented for examination in the School of Molecular and Biomedical Science. Parts of this thesis contain material of a commercially sensitive nature and may not be disclosed without prior consent of the author.

…….

Weiwei Tang

B.Sc. (Biotechnology)

July 31, 2013

ACKNOWLEDGEMENTS

I would like to extend my deepest gratitude to my supervisors, Associate Prof. Grant Booker and Dr. Steven Polyak, for your patient supervision, guidance and constant encouragement throughout this year. Thank you Grant for providing me opportunity to study in your lab, I really appreciate this experience, not to mention all your inspiring advice on both the experiments and presentations. Steven, thank you so much for all your enlightening talks and support, without you, I could not finish my exchange master program and the thesis in the present.

I would like to thank you Al for all the help in framing my project and help in experiments. Wanisa, it is a great pleasure to be your friend and you help me a lot to get used to a new culture environment. And a big thankyou goes to Ashileigh, for your help to get familiar with the new lab and for taking your time to read through my thesis. Jiulia, it is really enjoyable to eat chocolate with you and you are such a great labmate. To the other Booker lab members: Kate, Jorinda thank you for the help you have given me this year. I'd also like to extend thanks to Christopher McDevitt for giving advice on membrane protein purification, Miranda Ween for training me on ultracentrifugation and those advice on handling tricky membrane proteins, and Victoria Lewis for your wonderful advice (I always feel welcomed for asking questions).

My eternal gratitude also goes to my friends far and near, my familiy members who have supported me throughout this year. I will always love you. To Pengcheng Li and Lu Zeng who also involved in this program, I wish you two all the best with your future. Thank you Mama, for your patient listening and tolerating my bad temper when I feel discouraged. Thank you Dad, for always making me feel free and no burden. Being away from you two has been hard but you always make me feel beloved and never give me up.

ABSTRACT

.

ECF transporters are a group of newly defined ABC-like modular transporters and they are composed of three main elements: 1) a high-affinity membrane-embedded substrate binding protein (S component), 2) a membrane-spanning protein (T component), and 3) two identical or homologous ATPases (A, A' components) which resemble the nucleotide binding domains in ABC transporters. *Staphylococcus aureus* biotin transporter (*Sa*BioMNY) belongs to the subgroup II ECF transporters which are characterized by their shared use of energy coupling module (AT module) by several S components, with each having a different substrate preference. Therefore, characterizing the S families in ECF transporters are important for us to gain new knowledge about the mechanism of subgroup II ECF transporters. Besides, laboratory has developed a series of biotin analogues with antibacterial activity against *S. aureus*. Previous studies have demonstrated that these compounds were capable of binding to the S component of *S. aureus* (i.e. *Sa*BioY). It was reasonable to speculate that these biotin analogues were transported across the *S. aureus* cells by the biotin transporter BioY. To further improve the antibacterial potency and selectivity, the binding and translocation mode of these compounds across the bacterial membrane via *Sa*BioY needs to be defined.

By utilizing a filter disk diffusion assay, I determined that the susceptibility of *E. coli* BL21 to antibiotics (erythromycin, streptomycin and chloramphenicol) was significantly increased when wild type *Sa*BioY was heterologously overexpressed in the cells. A library of *Sa*BioY mutants was also screened in this assay and the overexpression of all the mutants surprisingly increased the sensitivity of *E. coli* cells to all three antibiotics compared to the un-induced one. One exceptional mutant was the D157K/K160E that was able to restore the tolerance of cells to the antimicrobial agents. I reasoned recombinant *Sa*BioY adopted a functional channel in the membrane of *E. coli* for low molecular weight antibiotics to diffuse through. In

addition, I also found that R75, D157 and K160 are essential to the surrogate transport pathway since a single amino acid change can dramatically alter the sensitivity of *E. coli* cells to antibiotics compared to the wild type one.

To further characterize the biotin core transporter *Sa*BioY, I attempted to purify recombinant *Sa*BioY from *E. coli* BL21 (DE3). The optimized conditions for expressing *Sa*BioY were determined to be 1) culturing cells at 25°C, 2) using the richer potassium buffered TB growth medium and 3) using a high concentration of IPTG (0.8 mM). I have also developed a system for the scalable purification of this integral membrane protein using SDS as a solubilizer. 9.7 mg of SDS-solubilized *Sa*BioY (with expected molecular weight of 19,492 Da) was obtained from 2 liters of culture after IMAC purification, with 90% purity determined by Commassie staining gel. A small panel of available mild detergents was subsequently tested for their efficiency of extracting membrane protein from natural lipids with TrionX-100 giving the best extraction efficiency. This present study paves the way for further detergent screening and purification of *Sa*BioY.

ABBREVIATIONS

ABC transporters	ATP-binding cassette containing transporters
ACC	Acyl-CoA carboxylase
Amp	Ampicillin
AMP	Adenosine monophosphate
ATP	Adenosine triphosphate
BioY	Biotin substrate binding protein
BioMNY	Intact biotin transporter
BPL	Biotin protein ligase
BSA	Bovine serum albumin
°C	Degrees Celsius
C-	Carboxyl-
CA-MRSA	Community acquired methicillin resistant *Staphylococcus aureus*
DMSO	Dimethyl sulfoxide
DNA	Deoxyribonucleic acid
DTT	Dithiothreitol
ECF	Energy-coupling factor
EDTA	Ethylene diamine tetra-acetic acid
g	Gram
HA-MRSA	Hospital acquired methicillin resistant *Staphylococcus aureus*
hSMVT	Human sodium-dependent multivitamin transporter
kDa	Kilo Dalton
LB	Luria broth
m	Milli-
M	molar

MDR	Multidrug-resistant
MCC	3-methylcrotonyl-CoA carboxylase
MCT1	Monocarboxylate transporter 1
Min	Minute, minutes
MW	Molecular weight
n	Nano-
N-	Amino-
NBDs	Nucleotide binding domains
OD_{xnm}	Optical density at x nm wavelength
PC	Pyruvate carboxylase
PCC	Propionyl-CoA carboxylase
PCR	Polymerase carboxylase
PMSF	phenylmethylsulfonylfluoride
*Sa*BPL	*Staphylococcus aureus* biotin protein ligase
SDS-PAGE	Sodium dodecyl sulphate polyacrylamide gel electrophoresis
SEM	Standard erroe of the mean
SMVT	Sodium-dependent multivitamin transporter
TB	Terrific broth
TBS	Tris buffered saline
TMDs	Transmembrane domains
Tris	2-amino-2-hydroxymethylpropane-1,3-diol
µ	Micro-
V	Voltage
VISA	Vancomycin intermediate resistant *Staphylococcus aureus*
VRSA	Vancomycin resistant *Staphylococcus aureus*
wt	Wild type

CHAPTER 1: INTRODUCTION

1.1 NEED FOR NEW ANTIBIOTICS

Antibiotic resistance in nosocomial and community acquired infections have been recognized as a major threat to human health by the World Health Organization. Bacterial pathogens, including Gram-positive bacteria *Staphylococcus aureus* and *Streptococcus pneumoniae*, Gram-negative bacteria *Escherichia coli* and *Helicobacter pylori*, are particularly important infectious microorganisms [1]. Antimicrobial agents have long been considered as powerful weapons to combat pathogenic bacteria. However, as more antibiotic-resistant strains are being reported, biochemists and pharmaceutical companies are facing a tough dilemma. Compared to the rapid emergence of multidrug-resistant (MDR) bacterial strain, the number of antibiotics being developed and licensed is far behind. In the past decade, only four new classes of antibiotics have been approved by the FDA [2]. The lack of innovation in the field of antibiotic development is largely attributed to the big pharmaceutical companies abandoning their research programs due to low commercial returns [3].

S. aureus was first identified in a study based on clinical observations published by Sir Alexander Ogston in 1882, and was classified into the *Micrococcaceae* family [4]. Humans are natural hosts for *S. aureus*. It was estimated that 20% of the human population are persistently colonized with *S. aureus* while even larger population (~60%) are transient carriers [5]. *Staphylococcal* infections can range from a minor skin infection, for example pimples, boils and abscesses, to life-threatening bloodstream infections which might result in sepsis and infective endocarditis [6]. *S. aureus* is the main cause of nosocomial infections for patients in intensive-care units and is also becoming a great concern in community settings as individuals with no recent surgery or hospital experience are contracting community acquired

Staphylococcal infections [7]. Due to inappropriate and excessive use of antimicrobial agents, *S. aureus* has developed resistance to a number of antibacterial agents, including β-lactam penicillin (e.g. methicillin) and vancomycin.

Methicillin-resistant *S. aureus* (MRSA) was first reported in 1961 in a British hospital 2 years following the introduction of methicillin [7]. Hospital-acquired MRSA (HA-MRSA) soon disseminated. The first case of community-acquired MRSA (CA-MRSA) was reported in Michigan, USA among drug abusers in the early 1980s [8]. The resistance mechanism employed by CA-MRSA is distinct from that of HA-MRSA, thereby making treatment more complicated and expensive [9]. For many years vancomycin was considered the antibiotic of last resort to treat MRSA. However, the emergence of vancomycin intermediate-resistant *S. aureus* (VISA, MIC for vancomycin of 8-16 mg/L) and vancomycin-resistant *S. aureus* (VRSA, vancomycin MIC ≥ 32 mg/L) has been observed in recent times [10]. The emergence of multidrug resistance *S. aureus* is in stark contrast to the number of new agents being developed to combat resistance. Therefore it is important for us to identify novel classes of antibiotics that are not subject to these current resistance mechanisms. Our lab focuses on the biotin biocycle from humans and major pathogenic bacteria with a view to exploiting essential metabolic activities as a route to finding new antibacterial chemotherapies. We have developed potent inhibitors against biotin protein ligase (BPL) that are based upon the natural ligand (aka biotin) used by the enzyme. As these compounds are biotin analogues, it is reasonable to propose that they cross the bacterial membrane using a biotin transporter. My project here is to characterize the putative transport protein BioY from *S. aureus*. This chapter will review recent literature around the structure and function of this transporter.

1.2 BIOTIN AND ITS BIOLOGICAL ROLE

Biotin (also named as vitamin H or B7) is a water-soluble molecule with the molecular weight of 244 Da. It serves as a coenzyme for the following four carboxylases in mammals: acetyl-CoA carboxylases (ACC1 and ACC2), pyruvate carboxylase (PC), 3-methylcrotonyl-CoA carboxylase (MCC) and propionyl-CoA carboxylase (PCC). ACC catalyzes the carboxylation of acetyl-CoA to form malonyl-CoA, which is the first committed step in acid biosynthesis. In mammals malonyl-CoA is also an allosteric inhibitor of the transporter that moves fatty acids into the mitochondria for β oxidation [11]. PC is involved in the formation of oxalacetate from its precursor pyruvate. This carboxylation reaction is pivotal for both gluconeogenesis and replenishing the Krebs cycle [12]. MCC and PCC both participate in the metabolism of certain amino acids [13, 14]. Biotin plays an essential role in carboxylase-dependent metabolism of fatty acids, glucose and amino acids in an indirect way.

1.3 BIOTIN UPTAKE IN MAMMALS BY SMVT AND ALTERNATIVE MCT1

As previously described, biotin is an important micronutrient in many cells. Therefore, it is important for biotin to be transported across cellular membranes. This is achieved by using a variety of transporters in different organisms. In this section I will discuss biotin transport in mammalian cells with a view to clarifying differences with the bacterial systems. Mammals are biotin auxotrophic and they must acquire the vitamin from exogenous sources such as from the diet and from intestinal microflora. It is well established that humans and other mammals absorb free biotin via the intestinal cells (**Figure 1.1**). This occurs through an efficient Na^+-dependent carrier-mediated mechanism. Intensive investigations into the human intestinal biotin transport system have found that the transporter is also responsible for translocating pantothenate (vitamin B5) and lipoic acid [15]. Thus,

the transporter has been named the sodium-dependent multivitamin transporter (SMVT). Human SMVT (hSMVT) consists of 635 amino acids and hydrophobicity analysis revealed that it contains twelve membrane spanning domains with both the amino- and carboxyl- termini facing towards the cytoplasm [16]. Currently no structural data has been reported for a mammalian SMVT.

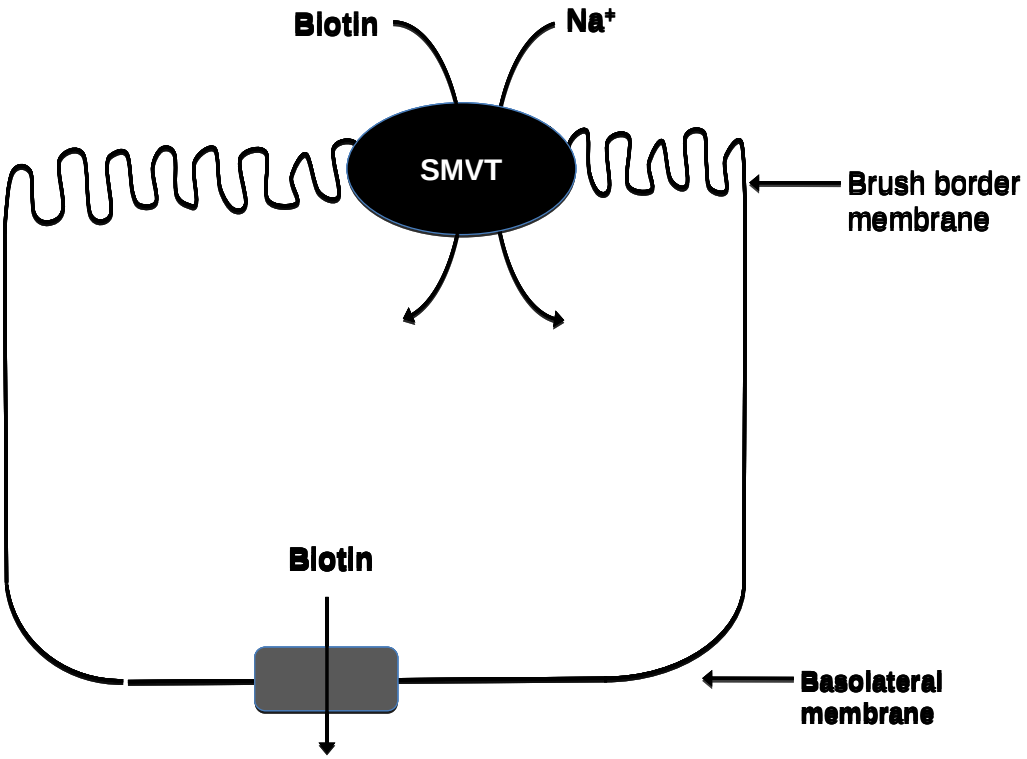

Figure 1.1: Illustration of biotin uptake in mammals by SMVT

Notwithstanding the well-defined role for SMVT in biotin uptake, there is growing evidence indicating that in lymphoid cells it is monocarboxylate transporter 1 (MCT1) that mediates biotin translocation. MCT1 demonstrates tissue preference of biotin transport and in other tissues, placental cells and lung cells for instance, there is no transport activity [17]. The reason for this phenomenon needs to be elucidated. MCT family is known for proton-linked transport of metabolically important monocarboxylates such as lactate, pyruvate, branched-chain oxo acids and ketone bodies [18]. Currently, nine MCT-related sequences have been identified with each having a unique tissue distribution [19]. Four isoforms (MCT1-MCT4) have been experimentally verified as lactate and pyruvate transporters. Previous studies

demonstrated that even though MCT1 mediates biotin uptake in immune cells, SMVT is still the major biotin transporter in mammalian cells [20].

1.4 GENERAL ARCHITECTURE AND TRANSPORT MECHANISM OF ABC TRANSPORTERS

The ABC transporters are a well characterized family of transport proteins. Investigations on ABC transporters have aided in understanding other modular solute transporters such as the biotin transporter. ABC transporters constitute one of the largest and most well characterized transporter superfamily. They are ubiquitously found in all three kingdoms and are widely recognized by their ability to couple ATP hydrolysis to the translocation of solutes against concentration gradients [21, 22]. ABC systems are involved in the uptake of nutrients, cell division, efflux of cellular waste products, as well as being notorious for causing multi-drug resistance in tumors and bacteria.

The fundamental organization of ABC transporter comprises two transmembrane domains (TMDs), providing the translocation pathway for substrates and two ATPase domains (also referred to as nucleotide binding domains, NBDs) that contribute energy to the transport system. For ABC importers, which are uniquely found in prokaryotes, an additional periplasmic soluble protein is required to facilitate substrate binding (named as SBP) [23]. The NBDs and TMDs in ABC importers reside on separate peptide chains whilst in ABC exporters they are usually fused into one chain and, therefore the two domains form a functional half transporter [24]. Several conserved motifs confer NBDs to contacting with TMDs and to coupling ATP hydrolysis reaction; 1) the Walker A (also referred to as phosphate binding loop), 2) Walker B, 3) signature motif (also referred to as C motif) that are in intimate contact with nucleotide; 4) the Q loop that is involved in interacting with TMDs [25]. It is noteworthy that dimeric NBDs assemble in a ‘head-to-tail’ arrangement. As a result, the Walker A motif of one NBD is in contact with the signature motif of the other subunit and between them the ATP-binding site

is sandwiched (**Figure 1.2**, [24]).

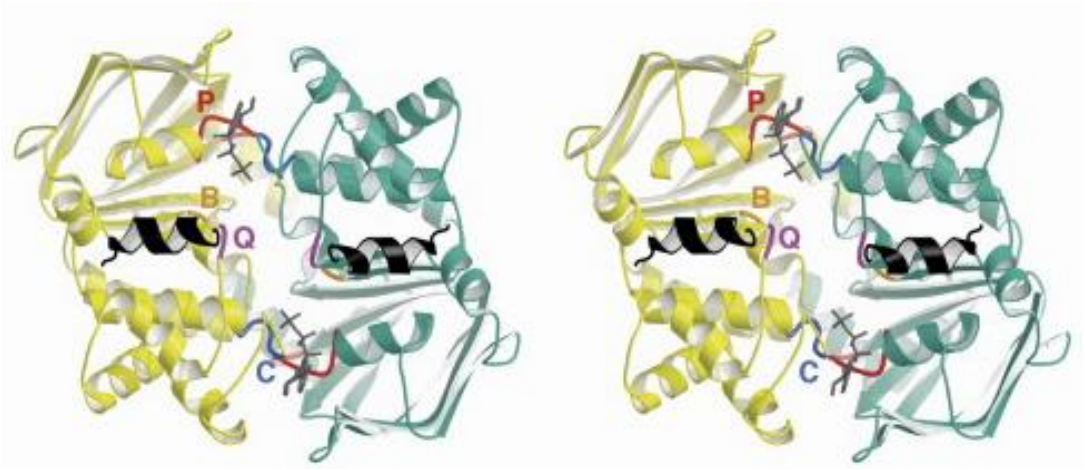

Figure 1.2: NBDs 'head to tail' arrangement [24]

NBD characteristic arrangement is represented by ABC exporter Sav1866 co-crystallized with ATP analogue and is illustrated from a membrane view with TMDs sit on top of them. The two NBDs are colored by yellow and green. Short, black helices indicate the coupling helices from TMDs. The sandwiched ATP analogues are shown in back sticks. P loop (P), Walker B motif (B), Q loop (Q) and Walker C motif (C) are colored by red, orange, purple, and blue, respectively.

Several X-ray crystal structures of ABC transporters have been solved. Structural information on the different liganded state of ABC transporter provides clues on the universal transport mechanism. A conserved feature is that the ATP binding to NBDs, and the subsequent hydrolysis event, are coupled to the conformational change in the TMDs. In the resting state (i.e. nucleotide free), the two NBD are apart and open. Once ATP binds to the nucleotide-binding site on each NBD, the two NBDs form a tightly bound dimer. This conformational change triggers the orientation change of TMDs from inword to outward (or outward to inward for exporters) coupled with the translocation of solutes. Following the release of AMP and inorganic phosphate, the complex switches back to the resting state (**Figure 1.3**, [26]). The coupling helices (the Q loop) on NBDs are identified as transmitting the energy information to TMDs [27].

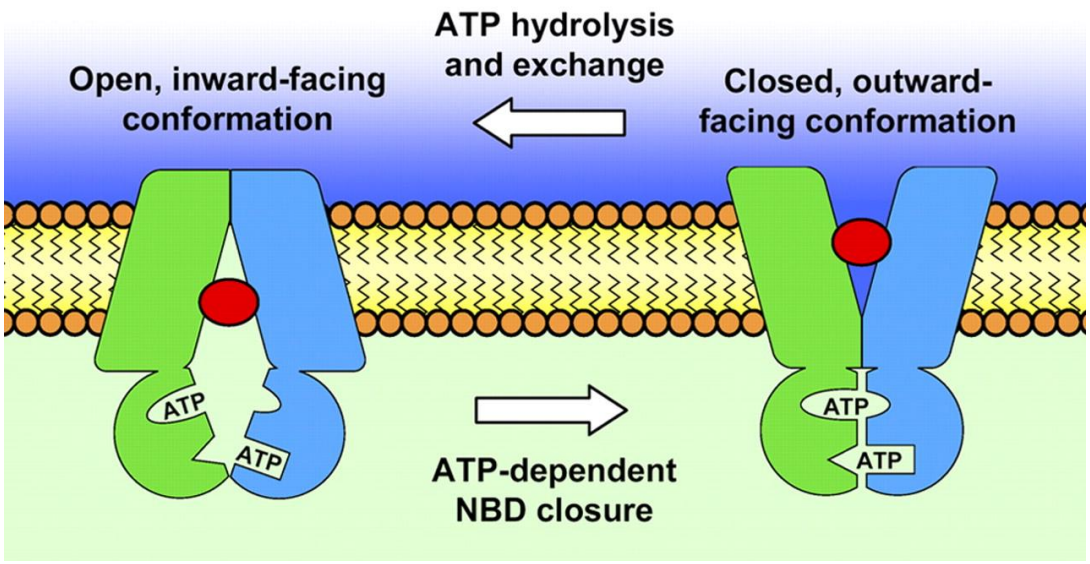

Figure 1.3: A universal transport mechanism for ABC superfamily [26]

ATP-dependent dimerization of intracellular NBDs promotes the facing direction change of TMDs (from inward to outward in this exporter model) followed by substrates translocation (red). Both exporters and importers are thought to generally adopt this transport mechanism [26].

1.5 ECF TRANSPORTERS, A NOVEL SUBGROUP OF ABC TRANSPORTERS

A combination of comparative analysis and experimental investigation enabled researchers to find that the biotin transport system (BioMNY) resembles the nickel and cobalt transport systems (NikMNQO and CbiMNQO, respectively) [28]. They all contain 1) a substrate binding protein which is embedded in the membrane, known as BioY for biotin, NikMN for nickel and CbiMN for cobalt; 2) an energy module which is composed of a soluble ATPase (BioM, NikO, CbiO) and a characteristic membrane-spanning permease (BioN, NikQ, CbiQ). These transport system responsible for vitamin precursors, vitamins and transition metal cations uptake are grouped into a novel modular transporter family, i.e. energy-coupling factor (ECF) transporter family [28].

ECF transporters share the similar modular architecture with that of most-dispersed ABC transporters. The representative ECF transporter consists of two identical or homologous nucleotide binding proteins (A, A' component or EcfA, EcfA') that are structurally similar to the NBDs of ABC transporters, a moderately conserved transmembrane protein (T component or EcfT) and a substrate binding protein (S component or EcfS). The A and T components together are also referred to as the energy-coupling factor module (ECF module). Although ECF systems resemble ABC transporters in respect of subunit composition they are still distinct in many ways (**Figure 1.4**, [29]). Firstly, the ECF transporters employ a membrane embedded protein to bind substrate instead of a soluble protein in ABC transport systems [30]. Secondly, the translocation pathways inside the ECF transporters are still controversial which indicates that the each subunit in ECF transporters might play a different role from their counterparts in ABC transporters.

ECF transporters fall into two groups depending on whether they employ a dedicated (subgroup I) or a shared (subgroup II) energy coupling module [31]. In subgroup I, the genes for the A-unit, T-unit and S unit are encoded in operons, exemplified by the biotin transporter BioMNY from *Rhodobacter capsulatus* [32]. In subgroup II ECF transporters (**Figure 1.3**, [29]), the S components for different substrates share a common coupling module in one organism. The genes for the AT modules of subgroup II tend to be encoded by operons. The latter is most commonly found in the phyla *Firmicutes* and *Thermotogales* and in some *Archaea* [28].

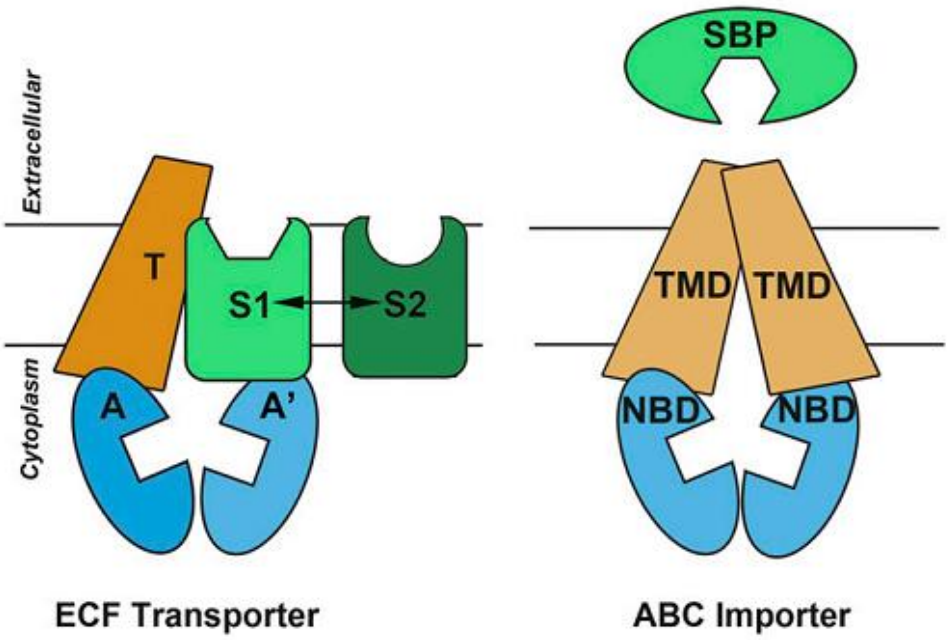

Figure 1.4: Typical architecture of ECF transporter (left) and ABC importers (right) [29]

ECF transporters employ a membrane-embedded protein to capture substrates, whereas ABC importers use a soluble substrate binding protein (SBP). Different S components of subgroup II transporters having different substrate specificity share the same energy coupling module (AT module) in one organism.

1.6 TRANSPORT MECHANISM OF ECF TRANSPORTERS

Our knowledge of ABC transporters helps us approach ECF transporters more efficiently since they are both ATP-dependent and possess same conserved motifs in ATPases [29]. From the two investigated quaternary structures of ECF transporters four components, A, A', T, and S, are believed to assemble with a 1:1:1:1 stoichiometry [29, 33]. Two helices from T component play a dominant role in coupling the S component with energy-coupling module. Five of the six helices in S component interact with T component through hydrophobic contacts. This structural feature is proposed to be essential for the interchange of S components with ECF. Based on a structural comparison between the hydroxymethyl pyrimidine

specific ECF transporter from *Lactobacillus brevis* and the ABC-type maltose importer, a model for ECF transporters was proposed by Yigong Shi group (**Figure 1.5**, [29]). In this model, substrate translocation is achieved through two major conformational changes. In the resting state, the ATPases EcfA and EcfA' are separated by a cleft. Upon binding ATP, the two subunits are pulled together promoting large changes in the coupling helices on EcfT. Conformational changes in EcfT allow EcfS to open outward and subsequently load the specific substrate. Following ATP hydrolysis and release of reaction products, the substrate is translocated. However, to substantiate this working model, the structures of the ECF transporters in different intermediate states need to be determined.

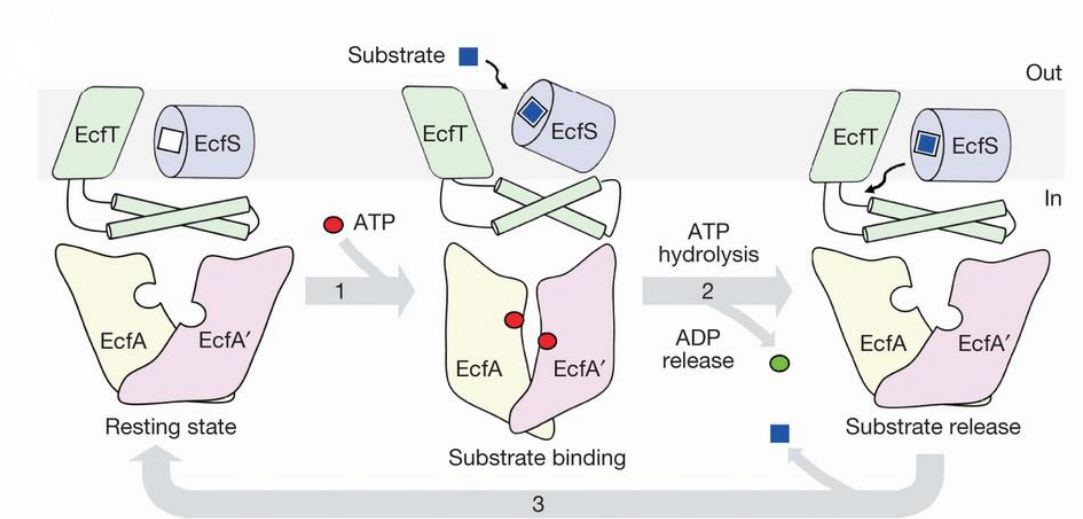

Figure 1.5: Diagrammatic illustration of potential transport mechanism for ECF transporter [29]

In this model, EcfA and EcfA' are open and apart in the resting state. ATP binding and hydrolysis pull the A and A' components form a tight heterodimer. The large structural changes are transmitted to EcfS through two coupling helices with a result of EcfS being substrate-loaded. The transport system is switched back to the resting state with the release of reaction products and substrate.

1.7 S components of ECF transporters

The S components, as the core transporter, are primarily responsible for determining the substrate specificity of ECF transporters. They are a group of small membrane proteins (~20kDa) with a large variation in their substrate preference [34]. Although their amino acid sequences differ between members from different S component families, their secondary structures are proposed to be conserved [29, 30, 34, 35]. Currently, crystal structures of three S components have been solved; riboflavin (RibU) from *S. aureus*, thiamin (ThiT) from *Lactococcus lactis,* and biotin (BioY) from *L. lactis* [34, 36]. Superimposed structures of *Sa*RibU, *Ll*ThiT and *Ll*BioY (**Figure 1.6**, [34]) reveal that the N-terminal domains are highly conserved while the C-terminal halves are more variable. The high conservation of N-terminal domains might explain their shared employment of the same ECF module in subgroup II.

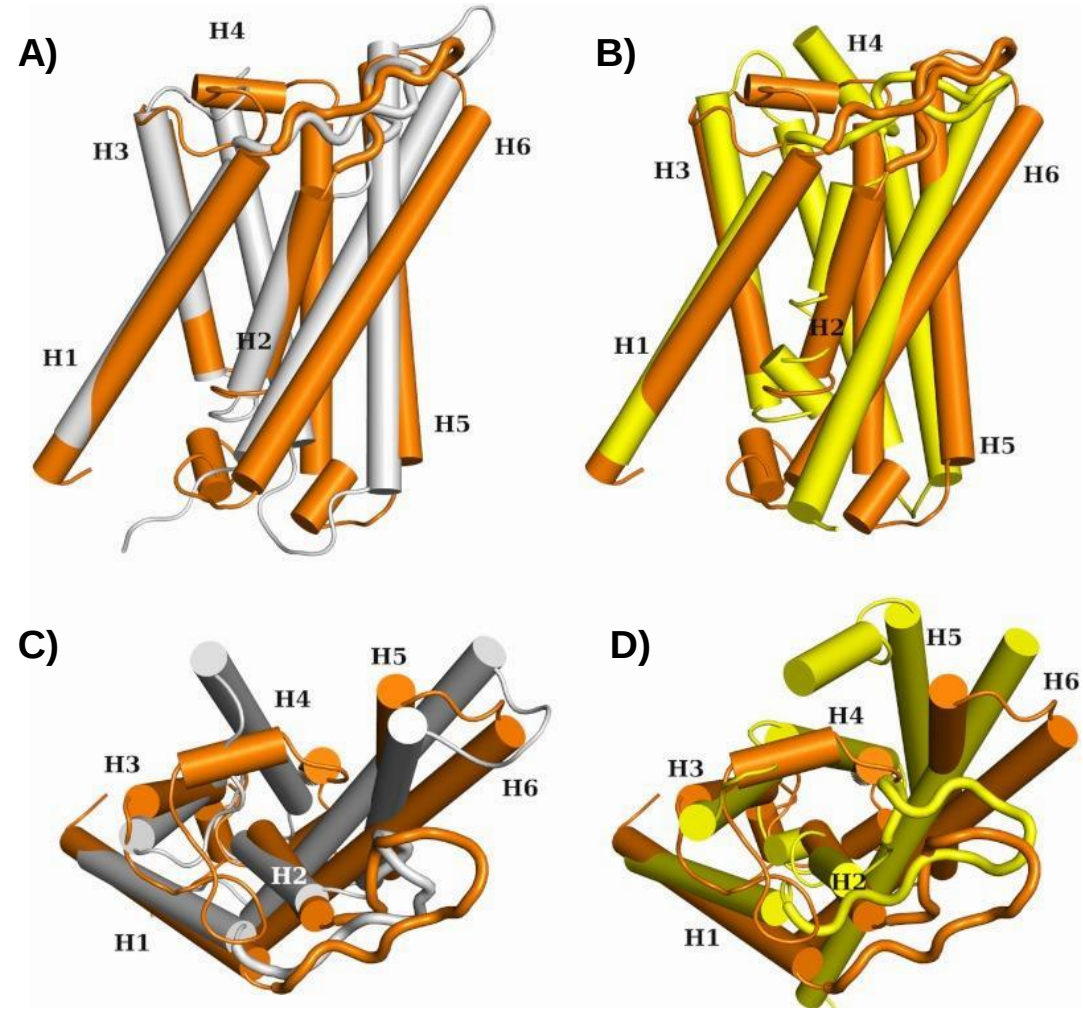

Figure 1.6: Superimposition of three S components [34]

The crystal structure of LlBioY (orange) was superimposed with either SaRibU (yellow) or LlThiT (grey). Panel A and B are depicted from the side view of the membrane, while C and D were shown as a view from above the membrane. Conserved helices 1-3 are superimposed across different S components. In contrast, helices 4-6 are variable. Loop 1 (between helix 1 and helix 2) illustrated in thick lines directly interacts with ligand.

1.8 BPL AND BIOTIN ANALOGUES

Biotin protein ligase (BPL) catalyzes the attachment of biotin onto biotin-dependent carboxylases in a two-step ordered mechanism as outlined in **Figure 1.7** [37, 38].

Biotinylation is carried out by first reaction between biotin and ATP with the product of an adenylated intermediate, biotinyl-5′-AMP. Biotinyl-5’-AMP stays bound to the biotin pocket of BPL until the ε-amino group of a conserved lysine residue on the biotin-dependent enzyme attacks the phosphoanhydride resulting in the formation of biotin covalently bound enzyme. The whole cyle of BPL-catalyzed biotinylation finishes with the release of AMP. Since BPL plays such a unique role in biotin-associated metabolic pathways, it presents a novel drug target for antimicrobial agent. Moreover, significant structural differences in the BPL between main pathogenic bacteria (for example *M. tuberculosis*, *E. coli* and *S. aureus*) and their human counterpart make it an attractive drug target [39]. Our laboratory has developed a series of biotin analogues mimicking the structure of the native biotinylation intermediate to inhibit *S. aureus* BPL (*Sa*BPL) activity, among which compound BPL-068 presents the most significant potency (K_i 90 nM) and high selectivity (>1100-fold) over its human homologue [40]. Our hypothesis is that these BPL inhibitors are transported cross the bacterial membrane via the biotin receptor. To better understand of this mechanism of solute import, further structure and function assays are required.

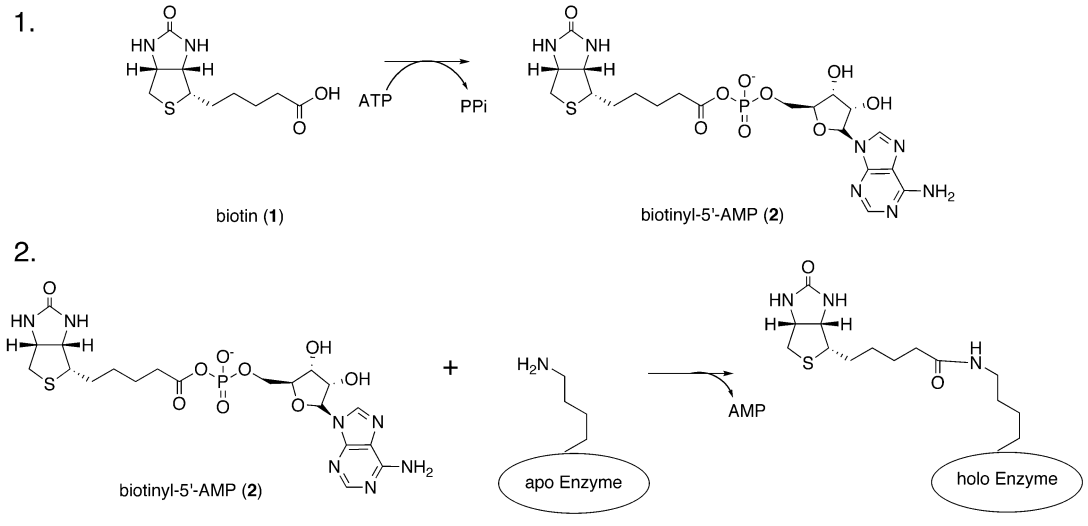

Figure 1.7 Two-step biotinylation reaction catalyzed by BPL [38]

1.9 Project aim and significance

Biotin is required by all three domains of life and can only be synthesized by bacteria, fungi and certain species of plant. For those biotin auxotrophic organisms, mammals for instance, biotin uptake from exogenous sources is essential. In mammalian cells, the most widely recognized transport system for biotin is SMVT. The prokaryotes distinguish themselves from mammals by utilizing a newly discovered ECF-type BioMNY transport system. This feature provides as an ideal drug target in terms of species selectivity.

S. aureus is able to synthesize biotin *de novo* as well as to transport biotin from outside of cells through an intact EcfAA'T-EcfS system. Prior studies in our laboratory confirmed that *Sa*BioY preferentially binds biotin. BPL inhibitors developed by our lab also showed binding activity which is exciting since it can be another starting point to improve the potency and selectivity of those compounds. To launch more functional and structural studies, heterologous expression and purification of this integral membrane protein is required.

CHAPTER 2: MATERIALS AND METHODS

2.1 MATERIALS

2.1.1 General Materials

Materials	Suppliers
CoStar 96 well round bottom clear plate	Corning Life Sciences, USA
Amicon® Centrifugal Filter Devices	Millipore, MA, USA
Ministart syringe filter 0.45 µm	Sartorius, Goettingen, Germany
Novex® Pre-cast gels	Invitrogen Life Technologies Inc., NY, USA
Pipette tips refill system	Eclipse, USA
50 ml precise syringe	BD, Australia/New Zealand
5 ml Profinia® IMAC cartridge	Bio-Rad Laboratories, Inc., CA, USA
PVDF membrane (Hybond™-C extra)	Amersham Pharmacia Biotech, CA, USA

2.1.2 Chemical reagents

All chemicals and reagents were of analytical grade or higher. Most common laboratory chemicals were purchased from Sigma Aldrich Inc. (St Louis, MO, USA) or BDH chemicals Ltd. (Victoria, Australia). Specialized reagents and their suppliers are listed below.

Reagents	Suppliers
2-log DNA ladder	New England Biolabs, MA, USA
Agarose, DNA grade	Probiogen Biochemicals, Australia
Bradford Protein Reagent Concentrate	Bio-Rad Laboratories Inc., CA, USA
Difco™ Vitamin Assay casamino acids	Becton, Dickinson and Company, MD, USA
DTT	BioVectra, Canada
D-glucose	Merck, Darmstadt, Germany
Gel Red® Nucleic Acid Stain	Biotium, CA, USA
IPTG	BioVectra, Canada
MES SDS running buffer	Invitrogen Life Technologies Inc, NY, USA
Seeblue®Plus2 Pre-stained Protein Marker	Invitrogen Life Technologies Inc, NY, USA
PMSF	Amresco

2.1.3 Restriction endonucleases

All restriction endonucleases, provided with appropriate buffers, were purchased from New England Biolabs, MA, USA.

2.1.4 Antibodies

Antibodies were reconstituted and stored as per manufactures instructions. Anti-6xHis antibody was supplied by Clontech Laboratories Inc., CA, USA. Cy3

conjugated AffiniPure Donkey Anti-mouse IgG was supplied by Jackson ImmunoResearch Laboratories, PA, USA.

2.1.5 Bacterial strains

***E. coli* BL21 (hsdS gal (λclts857) ind Sam7 nin5 lacUV5T7gene1):** *E. coli* BL21 carrying λDE3 insertion for expression of recombinant proteins using pET expression vector (Stratagene, La Jolla, CA, USA)

***E. coli* DH5α (*sup*EΔlac169 (p80lacZΔM15) hsdR17 recA1 end AA1 gyrA96 thi-1 relA1):** For routine molecular cloning (New England Biolabs, MA, USA)

2.1.6 Bacterial Media

Luria Broth (LB): 1% (w/v) tryptone, 0.5% (w/v) yeast extract, 1% (w/v) NaCl, adjusted to pH 7.0 with NaOH.

Terrific Broth (TB): 1.2% (w/v) tryptone, 2.4% (w/v) yeast extract, 0.4% (v/v) glycerol, 17 mM potassium phosphate monobasic, 72 mM potassium phosphate dibasic.

Minimum Supplemented Medium (MSM): 35 mM sodium phosphate buffer pH 7.0, 20 mM D-glucose, 37.5 mM NH_4Cl, 810 µM $MgSO_4$, 68 µM $CaCl_2$, 18.5 µM $FeCl_3$, 400 µg/mL casamino acid.

LB agar: LB supplemented with 1.5% (w/v) bacto-agar.

MSM agar: MSM supplemented with 1.5% (w/v) bacto-agar.

Bacterial selection: Selection of bacteria bearing plasmid was achieved through

addition of appropriate antibiotics to both liquid and solid medium. Ampicillin was used at 100 µg/mL of final concentration and kanamycin was used at 50 µg/mL of final concentration.

2.1.7 Commercial kits

Kit	Suppliers
QIAprep Miniprep Kit	QIAGEN, GmbH, Germany
QIAquick Gel Extraction Kit	QIAGEN, GmbH, Germany
BCA™ Protein Assay Kit	Thermo Fisher Scientific Inc., Rockford, USA

2.1.8 Buffers and Solutions

Blocking Buffer: 1% (w/v) BSA in PBS

Cell Lysis Buffer: 10% (v/v) β-mercaptoethanol, 2% (w/v) SDS

Cleaning solution 1 (2X): 100 mM NaCl, 100 mM Tris, at pH8.0

Cleaning solution 2 (4X): 2 M NaCl, 0.4 M sodium acetate, at pH 4.5

Coomassie blue stain: 0.2% (w/v) coomassie brilliant blue, 10% (v/v) ethanol, 10% (v/v) acetic acid

Coomassie destain: 10% (v/v) methanol, 10% (v/v) acetic acid

DNA loading buffer (6X): 0.5xTris-borate-EDTA (TBE) buffer, 40% (v/v) glycerol, 1 mg/ml bromophenol blue

Native IMAC wash buffer 1 (2X): 50 mM Tris at pH 8.0, 300 mM NaCl, 20% (v/v) glycerol, 20 mM imidazole

Native IMAC wash buffer 2 (2X): 50 mM Tris at pH 8.0, 300 mM NaCl, 20% (v/v) glycerol, 50 mM imidazole

Native elution buffer (2X): 50 mM Tris at pH 8.0, 300 mM NaCl, 20% (v/v) glycerol, 0.4% (w/v) SDS, 500 mM imidazole

SDS-PAGE loading buffer (5X): 0.25 M Tris at pH 6.8, 10% (w/v) SDS, 0.25% (w/v) bromophenol blue, 50% (v/v) glycerol

PBS-Tween: PBS, 0.1% (v/v) Tween20

TAE: 40 mM Tris pH 8.2, 20 mM sodium acetate, 1 mM EDTA

Transfer Buffer: 39 mM glycine, 48 mM Tris, 0.037% (w/v) SDS, 20% (v/v) methanol

2.1.9 Plasmids

pET16b was obtained from Dr. Steven Polyak (School of Molecular and Biomedical Science, University of Adelaide).

pAra13 (*Sa*BioY-H_6) was provided by Al Azhar (School of Molecular and Biomedical Science, University of Adelaide).

pUHA1 (*Sa*EcfAA'T) was provided by Al Azhar (School of Molecular and Biomedical Science, University of Adelaide).

2.1.10 Computer Software

Data were analysed by using GraphPad Prism 5 and Microsoft Excel 2010 software. Chemical structures were drawn using ChemDraw (version 10.0). Proteins blotted onto PVDF membrane were visualized using the Chemidoc (Bio-Rad).

2.2 METHODS

2.2.1 Protein Techniques

2.2.1.1 Preparation of cell lysate

For the preparation of whole cell lysates for SDS-PAGE analysis, 1 mL of culture was centrifuged at 6,200 x *g* for 3 min. The supernatant was discarded and the cell pellet was resuspended with 40 mL of cell lysis buffer per unit OD_{600}. Cell suspension was vortexed, spun and boiled at 95°C for 5 min, this process was repeated.

2.2.1.2 Determination of protein concentration

Protein concentration was assayed by using the Bradford Reagent (Bio-Rad Laboratories Inc., CA, USA). A standard curve of bovine serum albumin (BSA) was generated from zero to 1 mg/mL and a linear regression was used to calculate protein concentration. For the 1xBradford assay 10 µL of protein sample was mixed with 200 µL of Bradford Reagent in a 96 well plate (Corning Life Sciences, USA). Absorbance at 600 nm wavelength was measured on a microplate reader (Molecular Devices, CA, USA).

2.2.1.3 Western blotting

Proteins were transferred onto a PVDF membrane (Amersham Pharmacia Biotech) using a semi-dry transfer unit (Hoefer SemiPhor, Amersham Pharmacia Biotech). Six sheets of Whatman filter paper and the PVDF membrane were pre-soaked in Towbin Transfer Buffer prior to assembly of the gel sandwich. Proteins were transferred for 1 hour at 80 mA per gel. The membranes were then blocked in 1% (w/v) BSA blocking buffer for 1 hour at room temperature and washed 3 times with PBS-Tween. The membrane was probed with primary antibody (diluted in PBS-Tween) for 1 hour at room temperature and washed 3 times with PBS-Tween. The primary antibody used was anti 6xHis (diluted 1:1000) for detecting *Sa*BioY-H_6. The membrane was probed with secondary antibody (diluted in PBS-Tween) for 1 hour at room temperature and washed 3 times with PBS-Tween. The secondary

antibody used was Cy3 anti mouse (diluted in 1:5000). The probing was performed concurrently by using either both primary or both secondary antibodies and using a single membrane for each experiment. The blot was visualized using Chemidoc Imager (BioRad).

2.2.1.4 SDS PAGE and gel staining

Proteins were separated on a 4-12% Bis-Tris polyacrylamide precast gel (Invitrogen) under reducing conditions. Gels were electrophoresed at 200V in 1X MES SDS running buffer (Invitrogen). Gels were stained for at least 2 hours with Coomassie Blue stain before destaining with Coomassie destain at room temperature.

2.2.2 Molecular Biology Techniques

2.2.2.1 Agarose Gel Electrophoresis

Analysis of DNA and separation of DNA fragments was performed using agarose gel electrophoresis. Gel slabs were poured by melting 1.5% agarose (w/v) in TAE buffer. Prior to loading into wells, DNA samples were mixed with an appropriate volume of 6X DNA loading buffer. Samples were electrophoresed in TAE buffer at 100V and then stained in 1xGelRed™ nucleic acid gel stain solution for at least 10 min. DNA was visualized on a UV transilluminator and photographed using a Mitsubishi video processor.

2.2.2.2 Transformation

1-5 µL of plasmid was added to 200 µL of competent cells and incubated on ice for at least 30 min. This was followed by heat shock treatment at 42°C for 3 min followed by further 5 min incubation on ice. Cells were immediately plated onto

pre-washed LB agar plates with ampicillin selection.

2.2.2.3 Preparation of glycerol stocks

For long term storage of *E. coli* strains, equal volumes of an overnight culture and 80% (v/v) glycerol were mixed and stored at -80°C.

2.2.2.4 Plasmid Purification

For purification of plasmid DNA, the QIAGEN QIAprep Miniprep Kit was employed according to manufacturer's instructions.

2.2.2.5 DNA Sequencing

Plasmid DNA or PCR products were used as templates for DNA sequencing. A 20 µL reaction containing 200 ng DNA, 100 ng each of two appropriate primers, 1 µL of BigDye version 3 reaction mix (Perkin Elmer, Applied Biosystems, CA, USA) and 4 µL of 5X sequencing buffer for PCR. The PCR profile consisted of 30 cycles of denaturation at 96°C for 30 seconds, annealing at 50°C for 15 seconds and extension at 60°C for 4 min. After the thermocycling reaction, 80 µL of 75% (v/v) isopropanol was added to the PCR products, vortexed and incubated at room temperature for 30 min. Precipitated DNA was isolated by centrifugation at 24,000 x *g* for 20 min. The pellet was washed in 250 µL of 75% (v/v) isopropanol followed by centrifugation at 24,000 x *g* for 5 min and dried in a 37°C heating block. Sequencing was performed by the Molecular Pathology Sequencing Service at the institute of Medical and Veterinary Science, Adelaide using 3730 Analyser (Perkin Elmer, Applied Biosystems, CA, USA).

CHAPTER 3: HETEROLOGOUS OVEREXPRESSION OF *STAPHYLOCOCCUS AUREUS* BIOTIN TRANSPORTER SURPRISINGLY FACILITATES THE PENETRATION OF LOW MOLECULAR WEIGHT ANTIBIOTICS

3.1 INTRODUCTION

ECF transporters are a group of ABC-like modular transporters that are well-recognized for their roles in the uptake of transition ions and vitamins. Previous work in our laboratory has demonstrated that *S. aureus* BioY (YP_501014), recombinantly expressed on *E. coli* cells, functions as a high affinity biotin binding protein. However, it is still unknown whether orphaned BioY can transport solutes across biological membranes.

The permeation of antibiotics into Gram-negative bacteria has been well studied by several groups [41, 42]. Gram-negative bacteria characteristically possess an additional lipid bilayer, the outer membrane (OM). Like other biological membranes, OMs are highly impermeable to hydrophilic solutes due to the hydrophobic cores formed by alkyl tails. Outer membrane proteins (OMPs) often assume a β-barrel conformation and are found to take the responsibility of transporting various small molecular weight solutes across the membrane barriers [43]. Most characterized protein channels involved in antibiotic influx in Gram-negative bacteria belong to the nonspecific OmpF or OmpC superfamilies. Substitutions of a single amino acid in these porins can give rise to antibiotic resistant phenotypes [44, 45]. Clinical data have also attributed multi-drug resistance in Gram-negative bacteria to the changes in expression levels of porins, alteration of the types of porins that being expressed, mutations that disrupt the functional porin channel and, a possible mechanism by synthesizing channel-blocking organic molecules [46].

A detailed understanding of how antibiotics enter into bacteria may extend our

knowledge about complicated drug-resistance mechanisms and is of great importance for designing new antimicrobial agents. Here I demonstrate that the ECF-type biotin transporter BioY from *S. aureus* facilitates penetration of low molecular weight antibiotics into *E. coli* cells. We propose that this is due to a functional channel in the bacterial membrane formed for antibiotics to passively diffuse through.

3.2 SPECIFIC METHODS

3.2.1 Construction of *S. aureus* BioY heterologous expression system

The gene encoding *Sa*EcfAA'T was cloned into a low copy vector pUHA1, allowing expression of target protein under the control of IPTG. The plasmid contained the kanamycin resistance marker. The gene for *Sa*BioY-His_6 (or *Sa*BioY mutant) was inserted into pAra13 for arabinose inducible protein expression. This vector contained the ampicillin resistance marker. A library of *Sa*BioY variants were generated by Mr Al Azhar (School of Molecular and Biomedical Science, University of Adelaide). Mutants S85T, L68M/F106C, R75K, R75A, R75E, R75C, F143A, F143C, F29A, Insert, D128A, D128K, D157A, D157K, K160E, K160A and D157K/K160E were created using site-directed mutagenesis. The other mutants N38S, F88V, T54S/F81S, I139V/A152P, V80A/E109D, F177S were generated using random mutagenesis. Plasmids pUHA1-*Sa*EcfAA'T and pAra13-*Sa*BioY (or pAra13-*Sa*BioY mutant) were co-transformed into *E. coli* BL21 cells for heterologous expression.

3.2.2 Filter disk diffusion assay

Plasmids pUHA1-*Sa*EcfAA'T and pAra13-*Sa*BioY (or *Sa*BioY mutant) were co-transformed into *E. coli* BL21, followed by overnight growth with vigorous

shaking at 30°C in LB medium supplemented with 100 µg/mLof ampicillin and 50 µg/mL kanamycin. The pre-culture was diluted 1:50 into 20 mL of fresh LB medium supplemented with 100 µg/mL ampicillin and 50µg/mL kanamycin and grown at 37°C until the OD_{600} reached 0.8. Logarithmic phase culture (300 µL) was combined with 3 mL of molten 0.7% bacto agar (w/v) supplemented with 100µg/mL ampicillin and 50µg/mL kanamycin with or without inducing agents. The mixture was then spread onto corresponding solidified Minimum Supplemented Medium (MSM) agar plate, with or without the presence of inducing agents. The plates were left at room temperature for 10 min before a 6-mm specific-antibiotic-impregnated filter paper disk was applied. In the bacteria susceptibility tests, three antibiotics that target bacterial intracellular proteins were used **(Figure 3.1)**. They were erythromycin (50 mg/mL), chloramphenicol (20 mg/mL) both solubilized in 100% ethanol and streptomycin (200 mg/mLl) dissolved in sterilized ddH_2O. 100% ethanol impregnated filter disks were employed as a negative control. Plates were incubated at 37°C for 16 to 18 hours. The susceptibility of bacteria to antibiotics was evaluated by the inhibition zones formed around the antibiotic-impregnated disks. The data was plotted by using GraphPad Prism5 and experiments were carried out in biological triplicate. Error bars represent standard error of the means (SEM) of data. And p-value was carried out by applying unpaired t-test with 95% confidence intervals.

A)

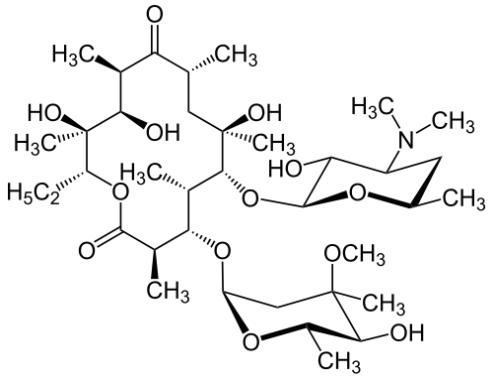

Erythromycin
MW 733

B)

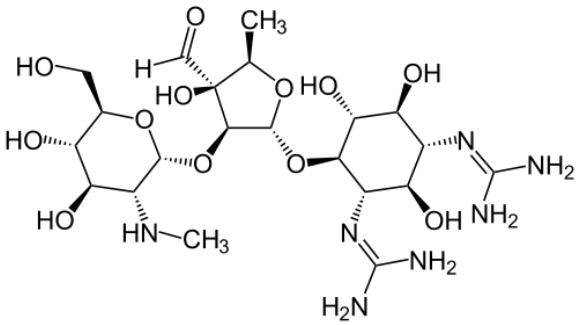

Streptomycin
MW 581

C)

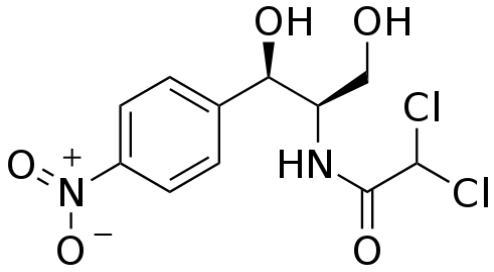

Chloramphenicol
MW 323

Figure 3.1: ChemDraw structures of the antibiotics tested in filter disk diffusion assay

3.2.3 Membrane fraction extraction

A single colony of *E. coli* BL21 harbouring pAra13-*Sa*BioY (D157K/K160E)-H_6 was picked and grown overnight in LB supplemented with 100 µg/mL ampicillin and 50 µg/mL kanamycin at 30°C. The pre-culture was diluted 1:50 into 50 mL fresh media and grown at 37°C until the OD_{600} reached 0.6-0.8. Arabinose (0.2%, w/v) was added to induce the expression of target protein. After 3 hours induction, the cell pellet was harvested by centrifugation at 6,200 x *g* for 10 min 4°C. Then pellet was resuspended with 3.5 mL of resuspension buffer (20% sucrose (w/v), 30 mM Tris-HCl at pH 8.0). Lysozyme, dissolved in 0.1 M EDTA at pH 7.3, was added to the resuspended mixtures followed by constant mixing at 4°C for 30 min until the mixtures were converted to spheroplasts. The cell mixtures were snap frozen in a dry ice and ethanol bath then thawed at room temperature for 30 min before being resuspended in 6 mL sonication buffer (3 mM EDTA at pH 7.3). The sonication was carried out at the 50-60% cycle for 15 seconds each time until the solution became homogenized. This and all the subsequent steps were performed at 4°C. Unbroken cells and cell debris were removed by centrifugation at 6,200 x *g* for 15 min. The supernatants from this low speed centrifugation step were further centrifuged at 150,000 x *g* for 1 hour to obtain the membrane fraction (pellet).

3.3 RESULTS AND DISCUSSION

3.3.1 Recombinantly expressed *Sa*BioY increased the susceptibility of *E. coli* BL21 (λDE3) to certain antibiotics

Initial experiments performed in the laboratory have demonstrated that *S. aureus* BioY can be recombinantly expressed on the surface of *E. coli* (Mr Al Azhar, unpublished data). Furthermore, this protein was shown to bind a fluorescent biotin tracer that can compete with biotin. However, it is uncertain whether biotin or other

biotin analogues can be transported across the *E. coli* cell membrane by *Sa*BioY. Here we propose a surrogate transport assay using a filter disk diffusion assay to determine whether the recombinant protein does form a functional channel for solutes to diffuse through. A small range of low molecular weight antibiotics that function via intracellular drug targets were tested. They were erythromycin (MW 733), streptomycin (MW 581) and chloramphenicol (MW 323) (**Figure 3.1**). The susceptibility of cells expressing *S. aureus* BioY to these antibiotics was quantified by measuring the inhibition zones around the antibiotic-impregnated filter disks. As indicated in **Figure 3.2A** and shown in **Supplementary Table 1** (at the end of this thesis), expression of wt *Sa*BioY significantly increased the susceptibility of *E. coli* BL21 to all three antibiotics as evaluated by significantly increased inhibition zones compared to un-induced cells. Moreover, the susceptibility of bacteria to antibiotics represented a positive correlation with the molecular weight of the agent. The smallest molecular weight chloramphenicol gave the largest inhibition zones in both induced group and un-induced group. In contrast, the data for erythromycin was less reproducible, possibly due to the larger molecular weight of this compound and its bulky side chains. To address whether the inducing agent, 0.4% arabinose (w/v), affected bacterial susceptibility to antibiotics, cells harbouring the parent plasmid pAra13 were investigated with streptomycin and chloramphenicol. As shown in **Figure 3.2B**, there was no significant difference in antibiotic sensitivity of cultures grown with or without arabinose. These data together indicated that the presence of *Sa*BioY increased the susceptibility of bacteria to these antimicrobial agents.

Previous studies on the ECF-type biotin transporter BioMNY from *Rhodobacter capsulatus* have shown that the presence of the BioMN could convert the core transporter (BioY) into a high affinity transport system [32]. It is reasonable to assume that the presence of BioY:EcfAA'T complex might make a difference on the susceptibility of bacteria to antibiotics compared to *Sa*BioY alone. Thus, IPTG was included in the growth medium to induce the expression of *Sa*EcfAA'T. It was observed that the expression of EcfAA'T caused bacteria to grow as isolated

colonies, rather than a clear lawn. I assumed this to be the result of toxicity caused by the overexpression of the membrane proteins. Therefore, I lowered the concentration of IPTG to 0.01 mM. Hence the experiment was carried out by supplementing the growth medium with 0.4% arabinose (w/v) and 0.01 mM IPTG. As shown in **Figure 3.2C**, no difference in susceptibility between BioY:EcfAA'T complex and solitary BioY was observed with all three antibiotics. Accordingly, all further experiments were performed using BioY alone and without EcfAA'T.

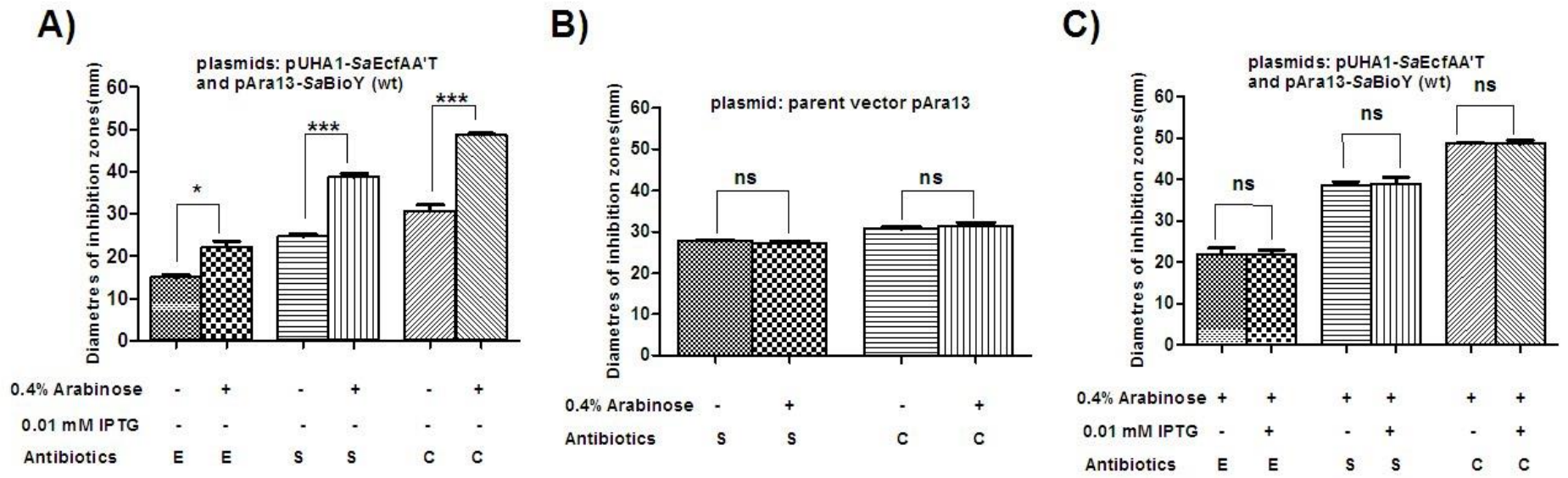
A)
plasmids: pUHA1-SaEcfAA'T
and pArá13-SaBioY (wt)
Diametres of inhibition zones(mm)
60
50
40
30
20
10
0
*
***
***
0.4% Arabinose - + - + - +
0.01 mM IPTG - - - - - -
Antibiotics E E S S C C
B)
plasmid: parent vector pAra13
Diametres of inhibition zones(mm)
ns
ns
0.4% Arabinose - + - +
Antibiotics S S C C
C)
plasmids: pUHA1-SaEcfAA'T
and pArá13-SaBioY (wt)
Diametres of inhibition zones(mm)
ns
ns
ns
0.4% Arabinose + + + + + +
0.01 mM IPTG - + - + - +
Antibiotics E E S S C C

Figure 3.2: Recombinant expression of *Sa*BioY increased the antibiotic susceptibility of *E. coli* BL21

*The expression of wild type (wt) SaBioY was induced by 0.4% arabinose (w/v) while 0.01 mM IPTG was used to induce the expression of SaEcfAA'T. The increased susceptibility of E. coli BL21 was determined by comparing the induced and un-induced groups in an individual antibiotic susceptibility test, as indicated in **panel A**. In both streptomycin (S) and chloramphenicol (C) tests, induced bacteria were much more sensitive to antimicrobial agent compared with the un-induced sample. In erythromycin (E) test, induced group also demonstrated significant difference from un-induced group. No significant difference in antibiotic sensitivity was observed between arabinose induced and un-induced cells as illustrated in **panel B**. The E. coli BL21 cells harbouring parent vector pAra13 were used here to expel the effects of inducing agent alone. Cells expressing SaEcfAA'T:BioY complex represented the same phenotype with those expressing BioY alone in antibiotic sensitivity, as demonstrated in **panel C**. * = p<0.05, *** = p<0.001, ns stands for no significant difference.*

3.3.2 Mutated *Sa*BioY altered the susceptibility of *E. coli* BL21 to antibiotics compared with wt *Sa*BioY

3.3.2.1 The positions of amino acid substitutions in a *Sa*BioY homology model

A model of *Sa*BioY was generated by A/Prof Grant Booker and Mr Al Azhar (School of Molecular and Biomedical Science, University of Adelaide) using the published crystal structures of ThiT from *L. lactis*, RibU from *S. aureus* and BioY from *L. lactis* (**Figure 3.3**). To further explore the molecular basis of *Sa*BioY as a membrane integrated substrate binding protein and its interaction with solutes, a series of *Sa*BioY mutants was designed to screen for amino acids required for binding activity. The positions targeted for site-directed mutagenesis (top panel of **Figure 3.3**) were determined upon several criteria; 1) F29 is conserved among the three revealed X-ray crystallographic structures of S components (*Ll*ThiT, *Ll*BioY and *Sa*RibU); 2) R75 is in GGRGG motif which is known to be important for biotin binding in BPL; 3) D128, D157, K160 are residues that are highly conserved among BioY families; 4) F143 and F106 substitutions were designed for cross linking experiment to explore the *Sa*BioY membrane topology; 5) S85 is in the AXXXA motif in *Sa*BioY which was predicted to be important for coupling with EcfT. Additionally, mutants were identified from a random mutagenic screen as indicated in the bottom panel of **Figure 3.3**. All mutagenesis experiments were performed by Mr Al Azhar and the mutants described in subsequent experiments were kindly provided by him.

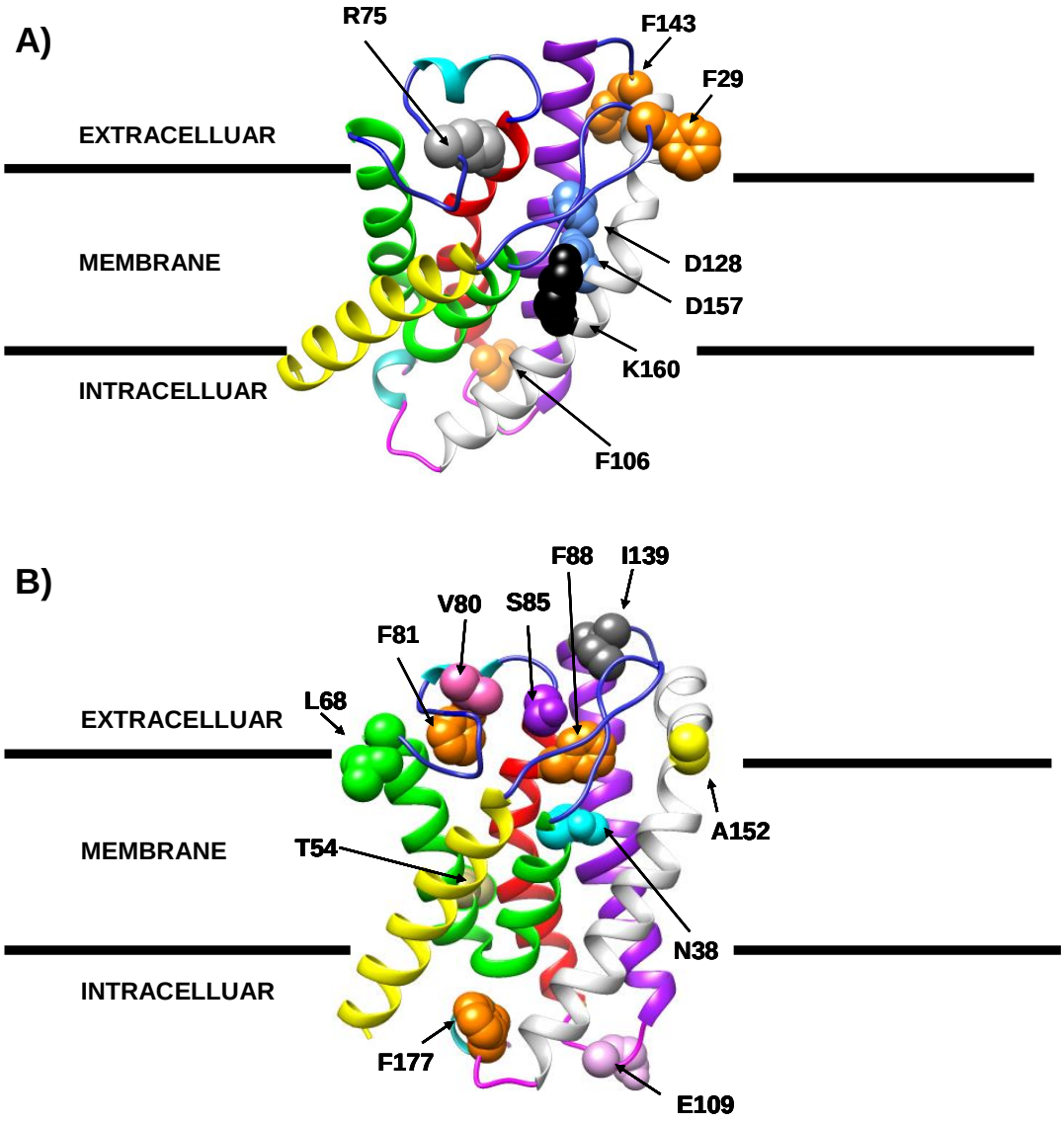

Figure 3.3: Positions of amino acid substitutions in a *Sa*BioY homology model

Helices 1-6 were represented by ribbons and colored by yellow (H1), green (H2), red (H3), sky blue (H4), purple (H5) and silver white (H6). Residues targetted for site-directed mutagenesis (A) and random mutagenesis (B) were represented by balls. Extracellular loop (dark blue) and intracellular loop (pink) were illustrated in thick lines.

3.3.2.2 The altered susceptibility of *E. coli* BL21 to antibiotics with the presence of individual *Sa*BioY mutant

In this study, the susceptibility of *E. coli* overexpressing *Sa*BioY mutants to antibiotics with the presence of individual *Sa*BioY mutant was investigated, and important residues were determined. The antibiotic sensitivity assay performed in 3.3.1 with wt *Sa*BioY was repeated with the panel of mutant proteins. For most mutants there was no significant difference from the wild type *Sa*BioY in the susceptibility to erythromycin, except D157K/K160E which was devoid of activity ($p<0.05$ vs wt) (**Figure 3.4B**). Comparing the diameters of inhibition zones produced by each antimicrobial agent, I surprisingly found that there was a significant difference in susceptibility between each induced *Sa*BioY mutant and corresponding un-induced sample. This suggested that all mutants were able to form a functional channel to allow the antibiotics to diffuse through. In all cases the double mutant D157K/K160E was an exception. For this mutant, the induced bacteria presented the same phenotype as the un-induced cultures. Strikingly, this same mutant dramatically lowered the susceptibility of *E. coli* BL21 to both streptomycin and chloramphenicol ($p<0.001$ vs wt) (**Figure 3.4D, 3.4F**).

Another mutant R75C also showed decreased susceptibility to both streptomycin and chloramphenicol ($p<0.05$ vs wt) (**Figure 3.4C, 3.4E)**. By contrast, F88V ($p<0.05$ vs wt), V80A/E109D ($p<0.05$ vs wt) and T54S/F81S ($p<0.01$ vs wt) increased the susceptibility of bacteria to both streptomycin and chloramphenicol. Interestingly, R75A ($p<0.05$ vs wt) significantly increased the susceptibility of *E. coli* BL21 to chloramphenicol (**Figure 3.5E**) while R75C was decreased.

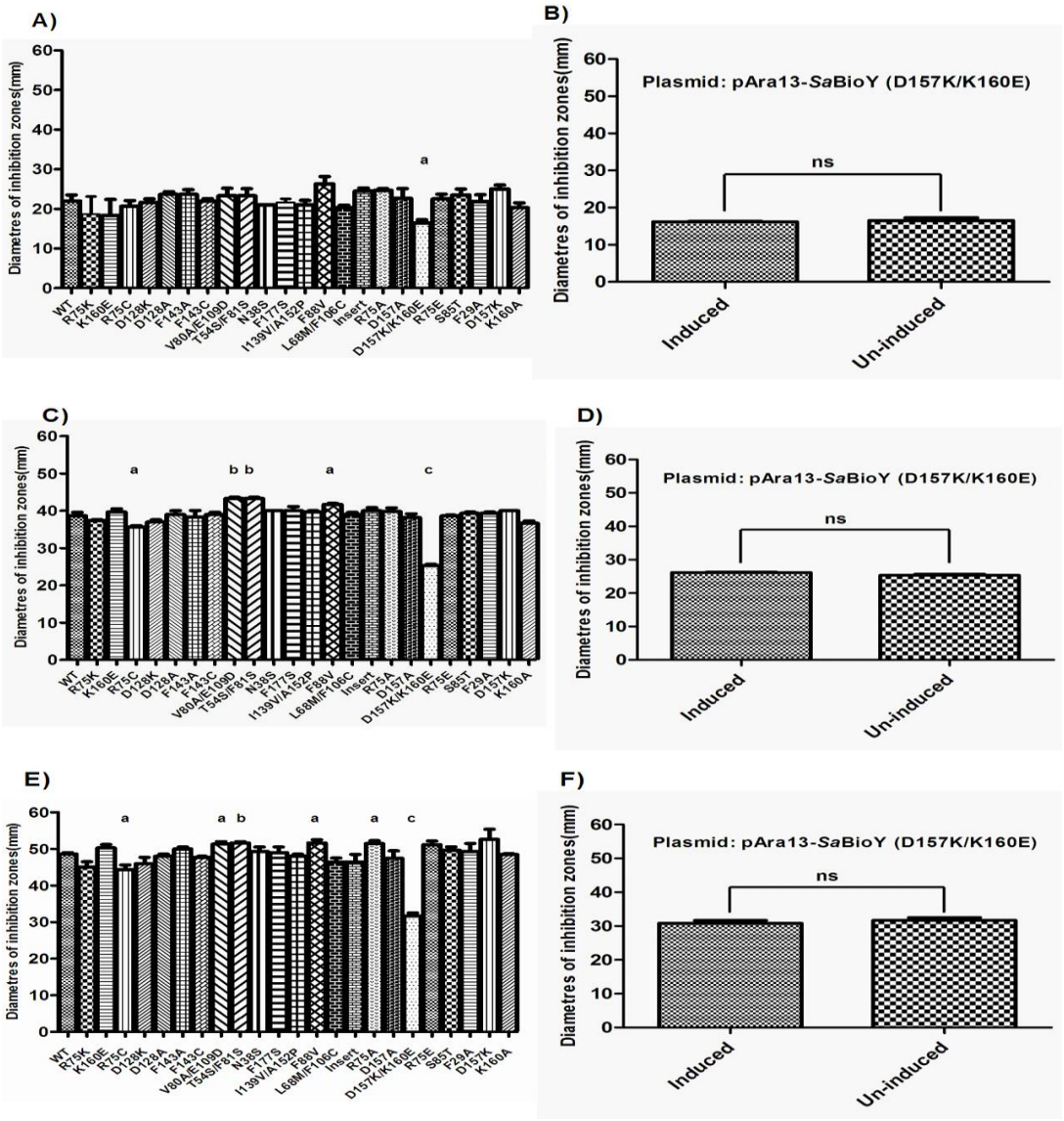

Figure 3.4: The susceptibility of *E. coli* BL21 to erythromycin (A, B), streptomycin (C, D) and chloramphenicol (E, F) with the presence of wt *Sa*BioY and mutants

*No significant difference was observed in the susceptibility of bacteria to all three antibiotics between induced D157K/K160E and correspondent un-induced group as shown in **panel B, D, F**. The susceptibility of bacteria to antibiotics with the presence of SaBioY mutants were shown in **panel A, C, E**. Inhibition zone of each mutant was compared with that of wt to evaluate the effect of amino acid substitutions (a=p<0.05, b=p<0.01, c=p<0.001 and ns stands for no significant difference).*

From these analyses, the double mutant D157K/K160E presented the most intriguing phenotype compared to the other mutants. To confirm expression of the protein in the bacterial membrane, Western blot analysis was performed on the soluble and membrane fractions of *E. coli* BL21 harbouring pAra13-SaBioY (D157K/K160E)-H_6 (as described in 3.2.3). Indeed, a bind of the expected size (19.5 kDa) was identified in the membrane fraction (**Figure 3.5**), suggesting that the expressed protein was targeted to the correct cellular fraction.

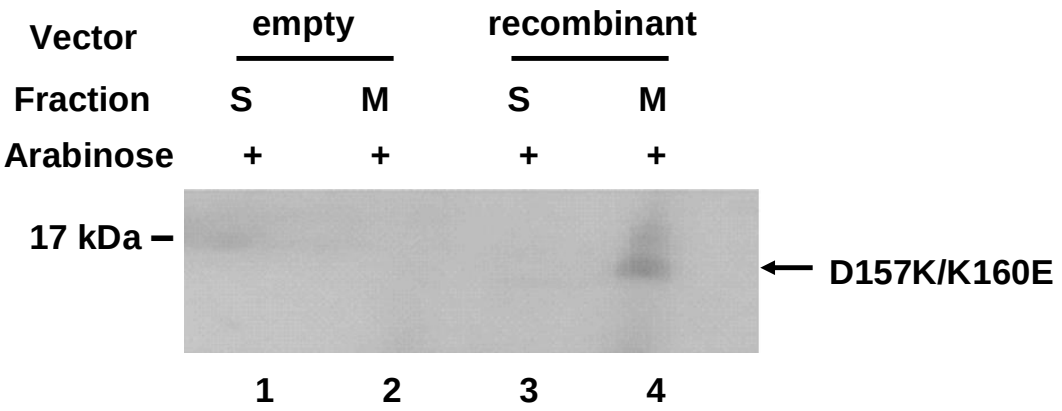

Figure 3.5: Anti-6×His western blot analysis to detect expression of D157K/K160E

SaBioY (D157K/K160E)-H_6 was constructed onto pAra13 and the recombinant plasmid was transformed into E. coli BL21. Parent vector pAra13 was used as a negative control. Expression of target protein was induced by 0.2% arabinose (w/v). Separation of membrane pellets from soluble proteins was carried out as described in 3.2.3. Different fractions after ultracentrifugation were loaded on the gel: soluble proteins (S) and membrane pellets (M). Right size band of SaBioY (D157K/K160E)-H_6 (as expected ~19 kDa) was detected in the membrane fraction (lane 4).

3.4 CONCLUSIONS

In this chapter, we explored the hypothesis that *Sa*BioY assembles as a functional channel in the membrane of *E. coli*. Indeed the data presented here supported the proposition that BioY serves as a pore for the passive diffusion of low molecular weight antibiotics into *E. coli*. We also screened a library of *Sa*BioY mutants and indentified amino acids R75, D157 and K160 as of particular importance for the penetration of these antibiotics into the cell.

CHAPTER 4: OPTIMIZATION OF HETEROLOGOUS OVEREXPRESSION AND PURIFICATION OF *STAPHYLOCOCCUS AUREUS* BIOY

4.1 INTRODUCTION

Membrane proteins are notoriously difficult to purify and to crystallize. Due to their hydrophobic nature, membrane proteins often tend to form insoluble inclusion bodies when recombinantly overexpressed in heterologous expression system. This has contributed to the reason why only a small number of crystal structures of integral membrane proteins have been solved compared to the large number of soluble proteins. In the early part of this chapter, I discussed the optimization of conditions for overexpression of *Sa*BioY on *E. coli*. I also demonstrated purification of *Sa*BioY by immobilized metal affinity chromatography (IMAC) using SDS as a solubilizing agent. As SDS is a denaturing detergent, it is not likely to be used in the protein functional and structural studies, but it can be used as a positive control for establishing a purification protocol. The later part of this chapter describes preliminary screening experiments using alternative detergents for extracting integral membrane *Sa*BioY from the bacterial membranes.

4.2 SPECIFIC METHODS

4.2.1 Recombinant *Sa*BioY expression

An overnight culture of *E. coli* BL21 (λDE3) harbouring pET-*Sa*BioY-H_6 were grown in TB medium supplemented with 100 µg/mL ampicillin at 30°C, then subcultured at 1:50 dilution into pre-warmed fresh medium containing 100 µg/mL ampicillin. The cells were grown at 37°C until OD_{600} reached 0.25 to 0.45. Subsequently the cultures were shifted to 25°C for 30 min prior to protein induction. Recombinant expression was induced with 1 mM IPTG for 14 hours at 25°C. The cells were

harvested by centrifugation at 6,200x *g* for 15 min at 4°C. The cell pellets were then resuspended in 50 mL of cell wash buffer (25 mM Tris-HCl at pH 8.0, 150 mM NaCl) per liter of cell culture. Cells were harvested by centrifugation at 6,200x *g* for 15 min and the weight of the cells was recorded. The cell pellets were again resuspended in 5 mL of cell lysis buffer (25 mM Tris-HCl at pH 8.0, 150 mM NaCl) supplemented with 1 mM final concentration of PMSF for each gram of cell pellet. Cells were disrupted by at least 5 passages through a M110L homogenizer (Microfluidics, USA). Unbroken cells and cell debris were removed by centrifugation at 24,000 x *g* for 30 min at 4°C. Membrane vesicles were collected by a subsequent ultracentrifugation at 150,000 x *g* (Beckman-Coulter Optima™ L-100 XP Ultracentrifuge, Rotor Type Ti 70.1), 4°C for 50 min. Membrane pellets were snap frozen in liquid nitrogen and stored at -80°C.

4.2.2 6xHis-tagged SaBioY purification

Membrane vesicles were thawed on ice and resuspended with 1 mL of solubilization buffer (25 mM Tris-HCl at pH 8.0, 150 mM NaCl, 10 mM imidazole, 10% glycerol, 2% SDS, 1 mM final concentration of PMSF) per gram of membrane pellet. The resuspended mixture was transferred into a 100-mL pre-chilled beaker and stirred by magnetic stone at room temperature for 1 hour. Insoluble material was removed by ultracentrifugation at 150,000 x g, 4°C for 50 min and the supernatant was collected for future work.

The purification was performed by using the default program method in the Profinia® purification system (Bio-Rad®), described here as follows. The supernatant fraction was applied at 10 mL/min onto a 5 mL Profinia® IMAC cartridge that was washed with 2 column volumes of milli-Q-water then pre-equilibrated with 5 column volumes of native IMAC lysis buffer (300 mM NaCl, 50 mM Tris-HCl at pH 8.0, 20 mM imidazole, 20% glycerol). The column was

washed with 6 column volumes of native IMAC wash buffer 1 (300 mM NaCl, 50 mM Tris-HCl at pH 8.0, 20 mM imidazole, 20% glycerol) followed by 6 column volumes of native IMAC wash buffer 2 (300mM NaCl, 50 mM NaCl at pH 8.0, 50 mM imidazole, 20% glycerol). H6-TEV-SaBioY was eluted with native elution buffer (300 mM NaCl, 50 mM Tris-HCl at pH 8.0, 500 mM imidazole, 20% glycerol, 0.4% SDS). Materials eluting from the column was detected by UV absorbance at 280 nm and pooled. The fractions containing SaBioY H6 were identified by western blot using an anti-6xHis antibody. The purity of the samples was assessed by SDS-PAGE.

4.2.3 Washing and recharging a 5 ml Profinia® IMAC cartridge column

The column was firstly washed with 5 column volumes of milli-Q-water (MQ-H2O), before bound Ni2+ was stripped off the resin by 5 column volumes of 50 mM EDTA. The column was then washed with 5 column volumes of MQ-H2O and treated with 5 column volumes of denaturing buffer (8 M urea or 6 M guanidine-HCl) before being washed again with 5 column volumes of MQ-H2O. The column was recharged with 2 column volumes of 50 mM NiSO4 and unbound Ni2+ was washed with approximately 5 column volumes of MQ-H2O. The column was equilibrated by Profinia® system in the practical practice as indicated above (section 4.2.2).

4.3 RESULTS AND DISCUSSION

4.3.1 Construction of pET16b-SaBioY-H6

pET16b (Novagen) was chosen as protein overexpression vector. Parent vector pAra13-SaBioY-H6 (provided by Mr Al Azhar, School of Molecular and Biomedical Science, University of Adelaide) was treated with restriction enzymes: NcoI and HindIII. After isolation of SaBioY-H6 gene, it was ligated into pET16b plasmid in preparation for DNA sequencing and protein expression. A restriction enzyme digest

was applied to determine whether the construct contained the desired gene. Eight colonies were picked for restriction digest analysis. Six colonies contained the correct size product and two colonies were selected for DNA sequencing for confirmation. The sequencing result of construct used in the subsequent experiments was shown in **Figure 4.1**.

Figure 4.1: DNA sequence analysis of construct pET-SaBioY-H6

The open reading frame (ORF) of SaBioY-H6 is indicated with red line at position 69 and 6xHis tag encoding sequence was indicated with red line at position 621.

4.3.2 Alternative way of detection of expression of SaBioY

The plasmid pET-SaBioY-H6 was transformed into E. coli BL21 (λDE3) for heterologous overexpression studies. Small scale expression studies were initially performed to identify clones that expressed SaBioY. Overnight cultures were used to inoculate 3 mL fresh LB containing 100 µg/mL ampicillin at 37 °C. Once the subcultures were in logarithmic phase, IPTG was added to a final concentration of 0.1 mM to induce protein expression. After 3 hours induction, whole cell lysates were prepared for analysis by SDS-PAGE. I could not see any difference between un-induced and induced samples on the Coomassie staining gel from this experiment (data not shown). Therefore I modified the protocol to improve detection of SaBioY. Firstly, expression was performed using larger cultures (50 mL) to increase the amount of protein. Secondly, cell fractionation (described in section 3.2.3) was performed to harvest the membrane fraction and enrich SaBioY. Thirdly, the concentration of IPTG was varied (0.2-0.8 mM). Also growth was performed at 37°C but for a longer time, 14hours. Finally, I employed western blot analysis using an anti-6xHis antibody to detect SaBioY-H6. Soluble proteins were removed by ultracentrifugation at 150,000 x g (as indicated in section 3.2.3) and membrane vesicles were dissolved with an appropriate volume of lysis buffer (2% SDS and 10% β-mercaptoethanol in MQ-H2O) at room temperature for 2 hours, taking care not to boil the samples as this can cause the aggregation and precipitation of membrane proteins. Western blot analysis revealed a band positioned between 17 kDa and 14 kDa as expected for SaBioY (**Figure 4.2**). Predicted SaBioY monomer runs faster than its expected molecular weight (19,492 Da) which was consistent with the behavior of BioY from Chlamydia Spp. [47]. At 28 kDa, a faint band predicted to be the SaBioY dimer was also detected. The optimal concentration of IPTG was determined as 0.8 mM (lane 6, **Figure 4.2**) and was applied in the following experiments.

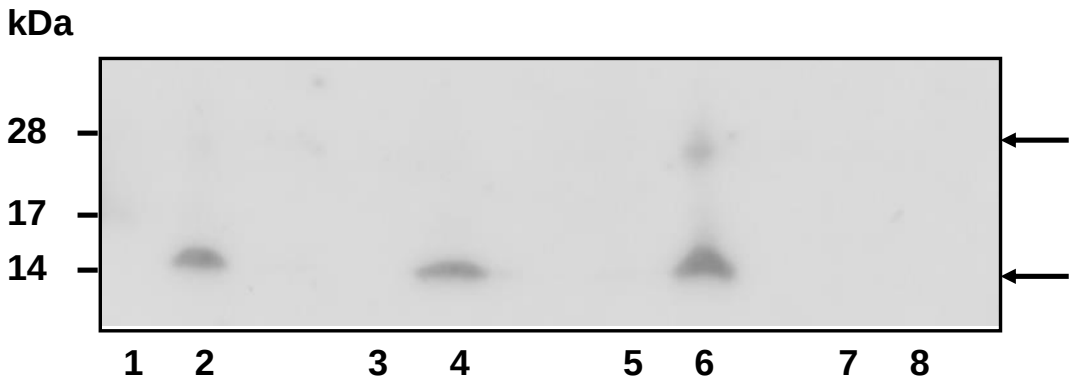

Figure 4.2: Detection of SaBioY by separating membrane fraction from soluble proteins

Cell fractionation was carried out by following steps indicated in section 3.2.3. The position of the predicted SaBioY monomer (~19 kDa) and SDS-resistant SaBioY dimer are indicated with black arrows to the right of panel. Samples loaded onto Lane1-6 were from cells harbouring pET-SaBioY-H6 induced by varied concentration of IPTG: lane 1: soluble fraction induced by 0.2 mM IPTG; lane 2: membrane fraction induced by 0.2 mM IPTG; lane 3: soluble fraction induced by 0.4 mM IPTG; lane 4: membrane fraction induced by 0.4 mM IPTG; lane 5: soluble fraction induced by 0.8 mM IPTG; lane 6: membrane fraction induced by 0.8 mM IPTG. Cells carrying parent vector pET16b were induced by 0.8 mM IPTG and fractions were separated as the same as of cells carrying recombinant plasmid. Samples from soluble part and membrane pellets were loaded onto lane 7 and lane 8, respectively.

4.3.3 SaBioY expression strain screening and optimization of culture medium

After repeating the above experiment several times, I observed that the protein expression was poorly repeatable. To improve the consistency of experiments I considered two variables: temperature and growth medium. Based upon the recombinant expression of YedZ [48], the growth temperature was first addressed. Once subcultures grown at 37°C reached early logarithmic phase they were

incubated at 25°C for 30 min before the addition of IPTG for inducing expression. Additionally, to buffer the acidic microenvironment produced by metabolicly active bacteria the LB medium was supplemented with 50 mM potassium phosphate at pH 7.0 and 0.5% glycerol. Terrific broth (TB) with richer nutrients and potassium phosphate buffer (medium recipe described in 2.1.2) was assessed alongside LB in this experiment. Five isolates were picked for expression strain screening (**Figure 4.3**). By comparing the amount of expressed protein in different strains cultured in different growth medium, optimal strain and expression condition for larger scale expression were determined. As can be seen in **Figure 4.3**, a predominant band at 28 kDa position was detected, with a secondary band between 17 kDa and 14 kDa detected in some samples. We speculated that the upper band was SDS-resistant SaBioY dimer while the lower one was SaBioY monomer. Generally, TB demonstrated to be more consistant compared with modified LB as bands in lane 4 and lane 5 were much weaker than the correspondent bands in land 9 and lane 10 (Figure 4.3). Isolate #1 cultured in TB as indicated in lane 6 (**Figure 4.3**) shows the best expression, so all further experiments were performed with this clone.

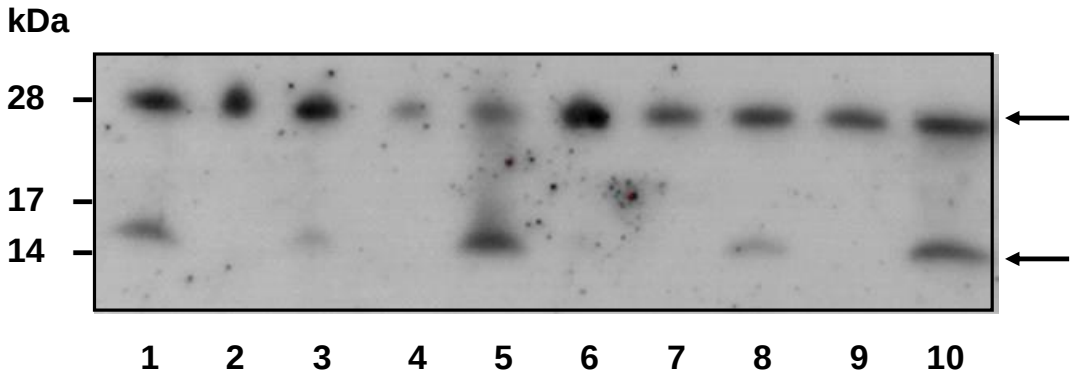

Figure 4.3: SaBioY expression strain screening

The plasmid pET-SaBioY-H6 was transformed into E. coli BL21 (λDE3) and 5 isolates were picked for expression strain screening. Same amounts of samples were loaded in all lanes for anti-6xHis western blot analysis. The position of the predicted SaBioY monomer (~19 kDa) and SDS-resistant SaBioY dimer are indicated with black arrows to the right of panel. Samples were loaded as below: lane 1: isolate #1 cultured in modified LB; lane 2: isolate #2 cultured in modified LB; lane 3: isolate #3 cultured in modified LB; lane 4: isolate #4 cultured in modified LB; lane 5: isolate #5 cultured in modified LB; lane 6: isolate #1 cultured in TB; lane 7: isolate #2 cultured in TB; lane 8: isolate #3 cultured in TB; lane 9: isolate #4 cultured in TB; lane 10: isolate #5 cultured in TB.

4.3.4 An established pipeline for scalable expression and purification of SaBioY

In the previous section I have optimized the recombinant expression of SaBioY. Next it was important to develop a protocol for the purification of this protein. SDS was used as the solubilizing detergent in this process. Protocol described in 4.2.1 section was followed by a larger scale expression. To obtain membrane fraction of E. coli BL21 (λDE3) during protein preparations, a number of centrifugation steps were applied as illustrated in **Figure 4.4A**. I routinely isolated the membrane fraction from

cell debris by ultracentrifugation. By separating the membrane pellets from the soluble proteins, membrane proteins were correspondently enriched as well as being protected from being degraded by soluble proteases. The ultracentrifugation steps were all carried out at 150,000 x g for 1 hour, allowing the soluble material to be separated from insoluble samples. As shown in **Figure 4.4B**, the purification of SaBioY-H6 was monitored by Western blot. As expected, target protein SaBioY-H6 accurately goes into the final soluble fraction (lane 6). SDS (2%, w/v) was used in this experiment even though it is not likely to be used in functional or structural studies. The proper way of manipulating multi-phase SDS is deeply discussed in section 4.3.5.

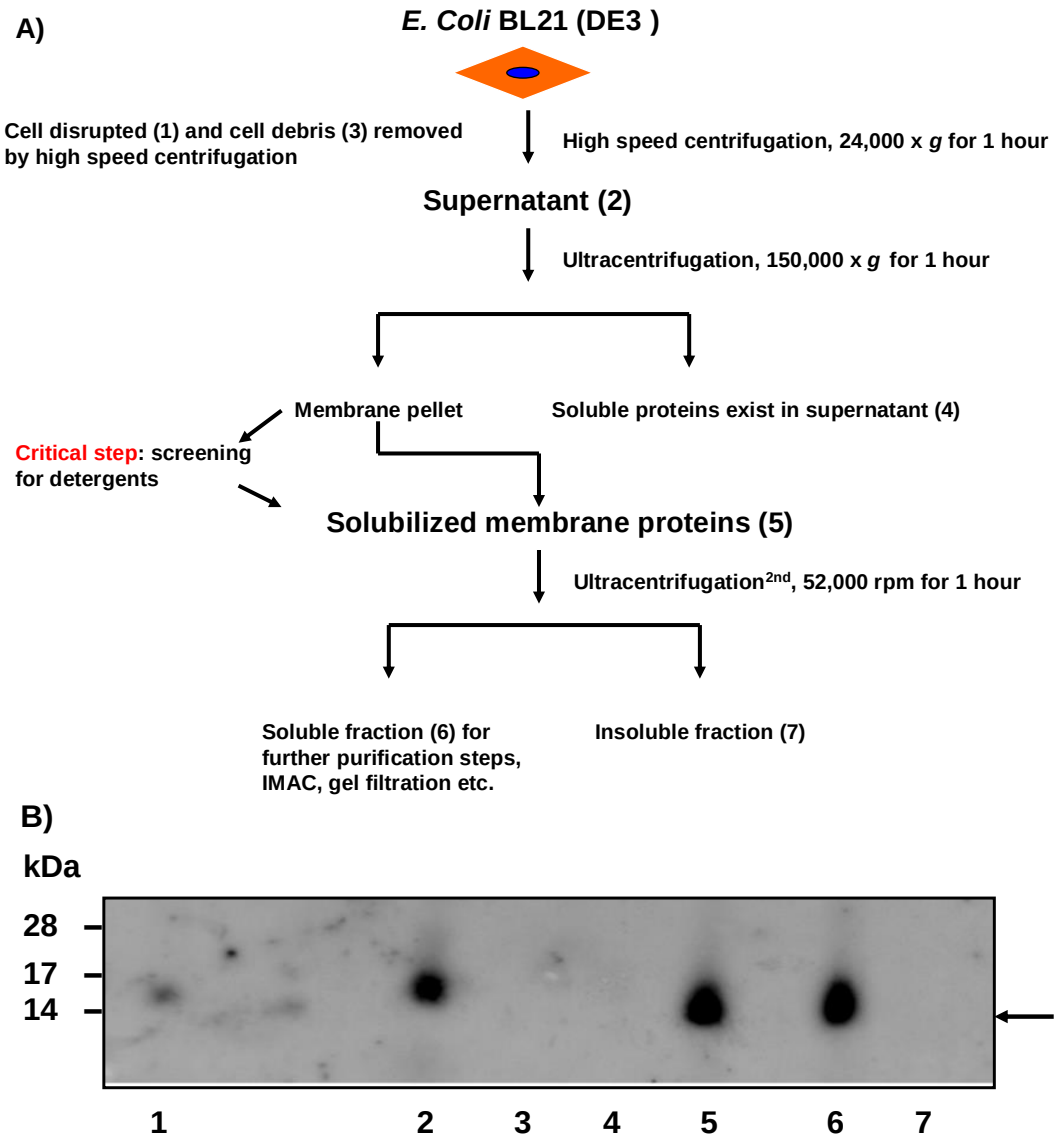

Figure 4.4: An established pipeline for obtaining soluble SaBioY

Solubilization and purification steps were established as indicated in panel A and purification of SaBioY was monitored by anti-6xHis western blot shown in panel B. Each labeled fraction was loaded onto the correspondent number of lane, lane 1: whole cell lysates; lane 2: supernatant after high-speed centrifugation; lane 3: unbroken cells or cell debris pellets after high-speed centrifugation; lane 4: supernatant to be discarded after the 1st ultracentrifugation; lane 5: membrane fraction to be solubilized by 2% SDS after the 1st ultracentrifugation; lane 6: supernatant after the 2nd ultracentrifugation; lane 7: insoluble pellets to be discarded after the 2nd ultracentrifugation.

4.3.5 Purification of SaBioY-H6 solubilized in SDS by IMAC

Before screening different detergents for their efficiency to solubilize membrane fractions, skillful manipulation of SDS used as the positive control, was required. Membrane pellets obtained from the 1st ultracentrifugation were dissolved using solubilization buffer (25 mM Tris-HCl at pH 8.0, 150 mM NaCl, 10 mM imidazole, 10% glycerol, 2% SDS, 1 mM final concentration of PMSF) and agitated at 4°C for 16 hours. However, white material mixed with insoluble pellets was observed after the 2nd ultracentrifugation. Most of SaBioY-H6 went into undesirable insoluble fraction as detected by anti-6xHis western blot (lane 6, **Figure 4.5**). The insolubility of SDS-SaBioY-H6 micelles was thought to be due to low temperature, causing the aggregation of SDS micelles. To make SDS coated SaBioY-H6 more dissolved, I then tried a much higher temperature 25°C for SDS solubilization and the following ultracentrifugation procedure. The successful application of this modified protocol was demonstrated in **Figure 4.4B**. Here I determined 25°C was optimal to manipulate multi-phase SDS. Empirical observations show that the SDS solubilization time can be reduced from 16 hour to 1 hour, providing a considerable advantage of ease and speed of processing the whole procedure.

To calculate the maximum yield and to evaluate the purity of target protein after inevitable immobilized metal affinity chromatography (IMAC) purification step, 2% SDS was employed to carry through the solubilization and purification steps. As shown in **Figure 4.6A**, SDS solubilized SaBioY were capable to bind the Ni^{2+} resin and was not prematurely eluted during the imidazole wash steps. 9.7 mg total protein from 2 liters culture was obtained. To make the band of elution fraction more visible on the Commassie blue staining gel, the eluate was concentrated by Amicon® Ultra 3K device (Millipore).

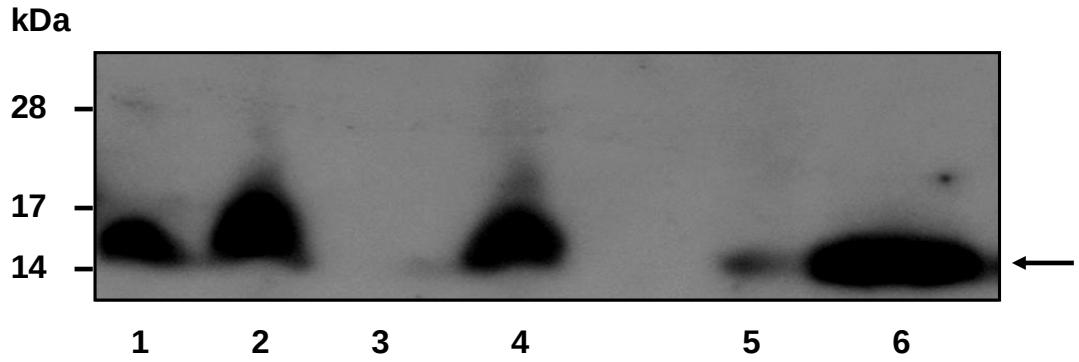

Figure 4.5: Solubilization of membrane pellets by using 2% SDS (w/v) at 4℃

Black arrow indicated the predicted SaBioY monomer (~19 kDa). Samples were from 2 liters cultures and loaded in different amounts. Samples were loaded as below: lane 1: whole cell lysate; lane 2: supernatant after high-speed centrifugation; lane 3: unbroken cells or cell debris pellets after high-speed centrifugation; lane 4: materials before the 2nd ultracentrifugation; lane 5: soluble fraction separated by the 2nd ultracentrifugation; lane 6: insoluble pellets after the 2nd ultracentrifugation.

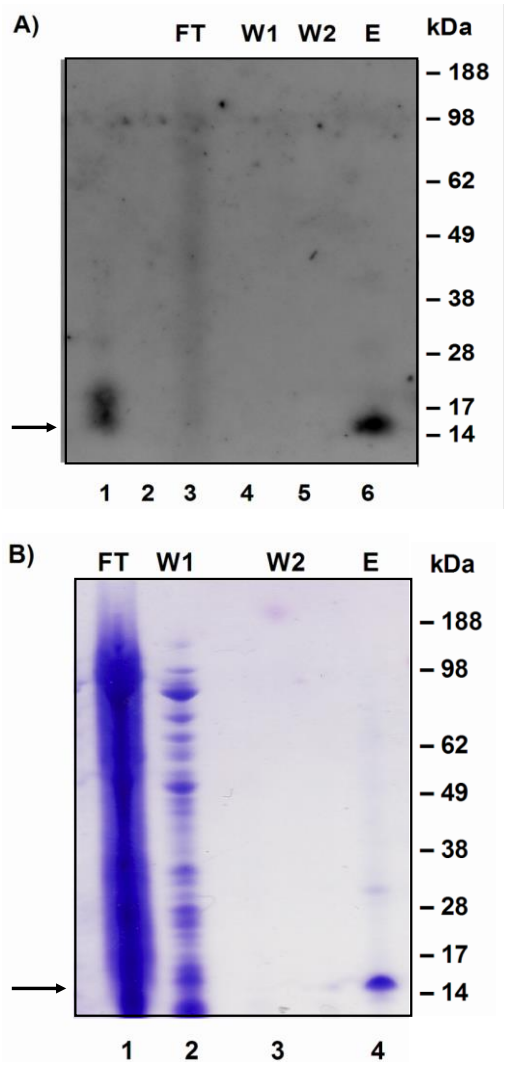

Figure 4.6: Purification of SDS solubilized SaBioY by using IMAC

The expression, solubilization and purification steps were carried out as described in section 4.2.2. Soluble fraction separated by the 2nd ultracentrifugation was loaded onto the Profinia® purification system (Bio-Rad). Various fractions were collected and run on separate 4-12% Bis-Tris polyacrylaminde gel (Invitrogen) for Coomassie blue staining and anti-6xHis Western blot analysis. Eluted SaBioY monomer was indicated with black arrows. Lane 1 of panel A contained the solubilized materials by 2% SDS (w/v) before the 2nd ultracentrifugation step. Lane 2 of panel A contained insoluble fraction separated by the 2nd ultracentrifugation. Various Fractions pooled from Profinia® system were indicated above the lanes; FT: flowthrough; W1: wash-1; W2: wash-2; E: eluate.

4.3.6 Detergents screening for solubilization of SaBioY

SDS is not ideal for functional or structural studies as it causes denaturation of the tertiary structure. Here, I needed to identify alternative detergents for the protein extraction. Membrane proteins need to be extracted from the lipid bilayer prior to the purification step. Detergents that can mimic the characteristics of lipid bilayer in shielding the hydrophobic membrane proteins are used in the solubilization process. Critical micelle concentration (CMC) is used to describe the aggregation property of detergent monomers. At concentrations below the CMC, the detergent exist as a monomer in solution while at concentration above the CMC, detergent monomers begin to self-associate to form micelles as illustrated in **Figure 4.7A** [49]. The identification of optimal concentration of detergent for the solubilization, purification or even crystallization is an empirical process. It is common to commence detergent screening at 2xCMC. Usually after the purification, membrane proteins are concentrated many fold before crystallization trials, resulting in an increased detergent concentration which might inhibit crystal formation in the following step. Dialysis of the concentrated protein is often employed to remove highly concentrated detergent. Detergents with higher CMC are much more dialyzable than detergents with a low CMC [50]. This property of detergents should also be taken into consideration when perform detergents screening.

A panel of detergents available in the laboratory was initially tested (**Table 4.1**; **Figure 4.7B**). To evaluate the efficiency of detergents in extracting membrane proteins from lipid bilayer, a comparison between the amounts of proteins in the soluble fraction versus insoluble fraction was required. An optimal detergent will solubilize all of membrane proteins such that no material should be detected in the insoluble fraction when analysed by Western blot. In the detergent screening experiment, SDS was used as a positive control as shown in **Figure 4.8 A** portion of SaBioY was detected in the soluble fraction using 1% (w/v) Triton X-100 and 1% (w/v) NP-40 while most of the protein remained in the unsolubilized fraction.

Optimized solubilization could be achieved by varying protein:detergent ratios, temperature, and solubilization time.

Table 4.1: Properties of desirable detergents

Detergent	Type	Agg.	MW monomer (micelle)	CMC mM (%w/v)	Dialyzable
Triton X-100	Nonionic	140	647(90K)	0.24(0.0155)	No
Tween 20	Nonionic	–	1228(–)	0.06(0.0074)	No
NP-40	Nonionic	149	617(90K)	0.29(0.0179)	No
CHAPS	Zwitterionic	10	615(6K)	8-10(0.5-0.6)	Yes
SDS	Anionic	62	288(18K)	6-8(0.17-0.23)	No

Agg. = Aggregation number, which means the number of molecules per micelle.

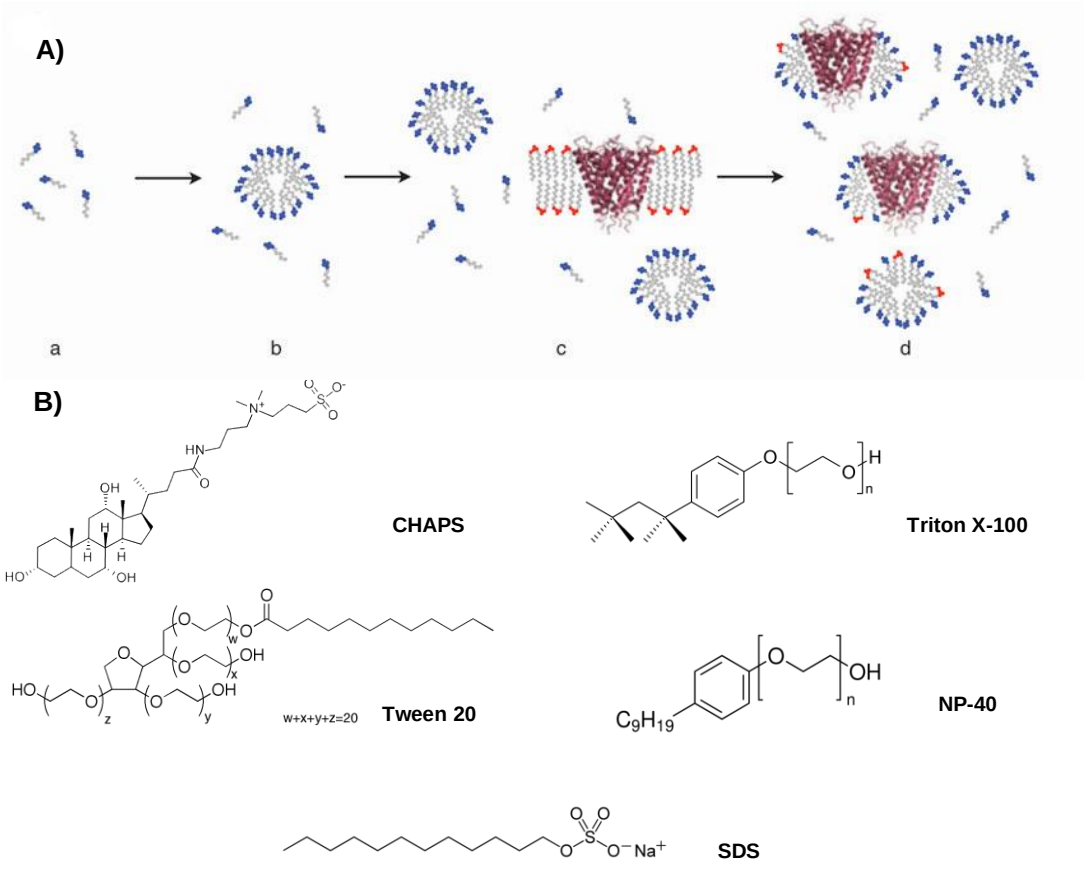

Figure 4.7: Detergent solubilization of membrane proteins

A) Schematic of the solubilization process, adapted from [49]. From left to right: detergent monomers (a) aggregate to form structures called micelles at the concentrations above CMC (b). When added to a membrane preparation, detergent monomers start to partition into membrane lipidbilayers (c) which results in mixed micelles including phospholipid-detergent micelles, detergent-protein micelles, and lipid-detergent-protein micelles during the extraction process (d) until all native membrane lipid:protein interactions are effectively replaced with detergent:protein interactions.

B) Chemical structure of detergents that have been tried.

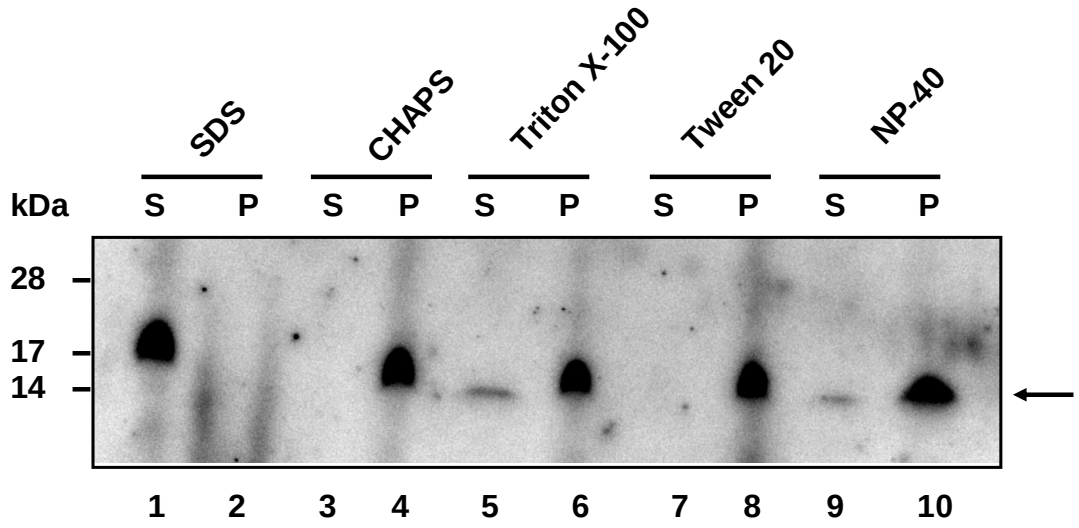

Figure 4.8: Efficiency of available detergents in solubilizing SaBioY

The membrane pellets were resuspended in 25 mM Tris-HCl at pH 8.0, 150 mM NaCl and total protein concentration was adjusted to 7.5 mg/mL. Solubilization was achieved by mixing 800 µL of membrane suspension with 400 µL of a 3% (w/v) detergent solution, giving a final detergent concentration of 1% (w/v). In the case of SDS and CHAPS were 2% (w/v) and 16 mM final concentration, respectively. After 1 hour solubilization at 4℃ (SDS was manipulated at 25℃), insoluble fraction was removed by miniultracentrifugation (Beckman-Coulter OptimaTM MAX-XP Ultracentrifuge) at 256,000 x g, 4℃ for 45 min. Soluble and insoluble fractions after this mini-ultracentrifugation were both collected and loaded with equal volume onto SDS-gel for anti-6xHis Western blot analysis. Predicted monomer SaBioY (~19 kDa) present in the soluble fraction was indicated with black arrows. Surfactants used in the solubilization were indicated above the lanes; S: soluble fraction; P: insoluble fraction separated by the mini-ultracentrifugation.

4.4 CONCLUSIONS

In this chapter, a workflow for expressing and purifying SaBioY has been devised. SDS-solubilized SaBioY from 2 liters cultures can achieve above 90% purity after the very initial IMAC purification step. We also have tried a small panel of available detergents to solubilize target protein, with Triton X-100 of being the most efficient one. Nevertheless, it is necessary to note that the protein activity after solubilization needs to be tested if further functional or structural studies are to be carried out.

CHAPTER 5: FINAL DISCUSSION AND FUTURE DIRECTIONS

5.1 FINAL DISCUSSION

ECF transporters are a newly discovered class of high-affinity modular transporters, responsible for uptake of vitamin precursors, vitamins and transition metal cations. They are uniquely found in prokaryotes. ECF-type biotin transporters, BioMNY, distinguish themselves from human biotin transporters (SMVT) in both architecture and transport mechanism which provides as an ideal feature for antimicrobial agent target. However, our knowledge about this newly identified transporter family still remains limited. Our laboratory has developed a series of potent BPL inhibitors against *S. aureus* that are reasonably proposed to be imported by BioMNY. Transport kinetic dynamics of the BPL inhibitors needs to be established if the antimicrobial potency of the compounds is to be improved. Taken together, it is necessary to characterize the core transporter *S. aureus* (*Sa*BioY) and purify the protein for further studies.

In the present study, I used a filter disk diffusion test to discover new potential role of the recombinant *Sa*BioY in antibiotics influx. The experiment was carried out in *E. coli* BL21 cells which have no *bioY* homologue gene. It was observed that with the presence of wt *Sa*BioY, the susceptibility of bacteria to erythromycin, streptomycin and chloramphenicol significantly increased ($p<0.05$) by approximately 50% for each antibiotic, relative to un-induced cells. Intriguingly a particular double mutant D157K/K160E significantly decreased the susceptibility of bacteria compared with wt *Sa*BioY. This finding is indicative of a functional channel formed by *Sa*BioY for low molecular weight antibiotics passive diffusion. D157 and K160 are residues highly conserved among BioY families, suggesting an important function role of these amino acids in the action of BioY. Individual substitution of these two amino acid sites (D157A, D157K and K160E) showed no alteration of bacterial sensitivity compared to wild type. However, simultaneously substituting both with opposite

charged amino acids significantly altered the *E. coli* cell phenotype, presenting a decreased sensitivity. According to the homology model (**Figure 3.3**), D157 and K160 are predicted to reside on helix 6 packed in the lipid membrane. I propose that these two residues act cooperatively through their side chains to facilitate the movement of solutes across the membrane to pass through. However, no pathway for solutes was found from the three X-ray structures of S component nor the BioY model [34]. This indicates a higher order complex, possibly a dimer or a trimer, is required for *Sa*BioY to function as a pore. Hence, the role of D157 and K160 is predicted to be stabilizing the higher order complex.

To further characterize this integral membrane protein, the expression and purification of recombinant *Sa*BioY was investigated and a workflow for obtaining soluble target protein was established. Integral membrane proteins are natively embedded in lipid bilayers, being protected from outer aqueous phase. Therefore, they are notoriously difficult to express, purify and crystallize. I optimized expression conditions by varying temperature, concentration of inducing compound (IPTG), and composition of medium. By lowering the induction temperature from 37°C to 25°C, I obtained consistent expression of the target protein. Also, using a richer growth medium terrific broth (TB) was shown to improve *Sa*BioY expression compared with modified LB medium supplemented with potassium phosphate buffer and glycerol. Subsequent large-scale preparation was performed using optimized conditions. To obtain membrane fraction containing target protein, several centrifugations were performed: 1) a low-spin centrifugation (6,200 x *g*) to harvest induced cells; 2) a high-speed centrifugation (24,000 x *g*) to remove cell debris and unbroken cells; 3) 1st ultracentrifugation (150,000x *g*) to pellet membrane fractions; 4) 2nd ultracentrifugation (150,000x *g*) to remove insoluble materials. SDS was used as positive control to solubilize the membrane pellets during the process of establishing a workflow. Approximately 10 mg SDS-solubilized *Sa*BioY from 2 liters cultures could be purified to >90% purity using a single IMAC purification step. This is a very promising result and it provides us with confidence that enough protein could be

produced for X-ray crystallography studies. Given that the entity of membrane protein crystal is a protein-detergent-complex (PDC), selection of the right detergent is critical [51]. I established the protocol for screening detergents for the protein purification step and also tried a small panel of laboratory available detergents. Here TritonX-100 proved to be the most efficient one. By varying conditions for detergent solubilization, temperature, buffer, detergent:protein ratio for example, the extraction efficiency of TritonX-100, CHAPS, NP-40 could be further improved. Here, having a homogeneous preparation of detergent is an advantage for crystallography. However, TritonX-100 is often a mixture of components, so that it is generally not preferred over more pure non-ionic hydrocarbon agents [52].

5.2 FUTURE DIRECTIONS

The bottleneck encountered in membrane protein structural studies is the extraction of target protein from membrane phospholipids and purification of suitable quantities for crystallography trials. A delicate balance, between reconstituting protein:lipid interactions with an appropriate detergent without causing the inactivation of target protein, should be considered when determine the optimal detergent. The identification of an optimal detergent must be performed empirically through trials with panels of candidate reagents. This will need to be performed next. However, there are some general trends that could help guide detergent selection. Nonionic and zwitterionic detergents are the two classes most used in structural studies. Nonionic detergents are those surfactants that contain polyoxyethylene or glycosidic head groups and are generally mild and non-denaturing. Nonionic detergents with short (C_7-C_{10}) hydrocarbon chain are frequently reported to inactivate target protein, such as octylglucoside and C_8E_4 or C_8E_5 [53]. It is noteworthy to mention that Dodecyl-β-D-maltoside and n-Dodecyl-β-D-maltoside are increasingly used in membrane protein solubilization. For example, in the case of a recently resolved quaternary structure of hydroxymethyl pyrimidine ECF-type transporter from *L. brevis*, proteins were solubilized in Dodecyl-β-D-maltoside. Zwitterionic detergents

exemplified by dodecyldimethyl-*N*-amineoxide are generally more inactivating than that of nonionic detergents. However, dodecyldimethyl-*N*-amineoxide has been successfully employed in structural studies of reaction center and mammalian rhodopsin. Steroid-based CHAPS also belongs to zwitterionic detergent. Nevertheless, its rigid steroid nucleus can retain protein activity in the detergent solubilized state which prevents its employment in structural studies.

Once the optimal detergent for extracting *Sa*BioY is determined, the purification of the protein based on the workflow I have established can be pursued. To investigate the transport kinetic dynamics of biotin and biotin analogues mimicking the natural environments, the purified *Sa*BioY is to be reconstituted onto phospholipids. In the reconstitution step, other detergents different from the extraction detergent can be considered to the advantage of the detergent property. Another long-term direction is to try to crystallize this membrane protein to gain a better knowledge about the subgroup II ECF transporters in *S. aureus*. All of the present studies will provide an approach to characterize this newly defined biotin transporter.

REFERENCES

1. Bakheet TM, Doig AJ: **Properties and identification of antibiotic drug targets**. *BMC Bioinformatics* 2010, **11**:195.
2. Cooper MA, Shlaes D: **Fix the antibiotics pipeline**. *Nature* 2011, **472**(7341):32.
3. Alanis AJ: **Resistance to antibiotics: are we in the post-antibiotic era?** *Arch Med Res* 2005, **36**(6):697-705.
4. Ogston A: **Micrococcus Poisoning**. *J Anat Physiol* 1882, **17**(Pt 1):24-58.
5. Kluytmans J, van Belkum A, Verbrugh H: **Nasal carriage of Staphylococcus aureus: epidemiology, underlying mechanisms, and associated risks**. *Clin Microbiol Rev* 1997, **10**(3):505-520.
6. Corey GR: **Staphylococcus aureus bloodstream infections: definitions and treatment**. *Clin Infect Dis* 2009, **48 Suppl 4**:S254-259.
7. Lowy FD: **Antimicrobial resistance: the example of Staphylococcus aureus**. *J Clin Invest* 2003, **111**(9):1265-1273.
8. Levine DP, Cushing RD, Jui J, Brown WJ: **Community-acquired methicillin-resistant Staphylococcus aureus endocarditis in the Detroit Medical Center**. *Ann Intern Med* 1982, **97**(3):330-338.
9. Appelbaum PC: **MRSA--the tip of the iceberg**. *Clin Microbiol Infect* 2006, **12 Suppl 2**:3-10.
10. Tiwari HK, Sen MR: **Emergence of vancomycin resistant Staphylococcus aureus (VRSA) from a tertiary care hospital from northern part of India**. *BMC Infect Dis* 2006, **6**:156.
11. Abu-Elheiga L, Matzuk MM, Abo-Hashema KA, Wakil SJ: **Continuous fatty acid oxidation and reduced fat storage in mice lacking acetyl-CoA carboxylase 2**. *Science* 2001, **291**(5513):2613-2616.
12. Jitrapakdee S, St Maurice M, Rayment I, Cleland WW, Wallace JC, Attwood PV: **Structure, mechanism and regulation of pyruvate carboxylase**. *Biochem J* 2008, **413**(3):369-387.
13. Baumgartner MR, Almashanu S, Suormala T, Obie C, Cole RN, Packman S, Baumgartner ER, Valle D: **The molecular basis of human 3-methylcrotonyl-CoA carboxylase deficiency**. *J Clin Invest* 2001, **107**(4):495-504.
14. Kalousek F, Darigo MD, Rosenberg LE: **Isolation and characterization of propionyl-CoA carboxylase from normal human liver. Evidence for a protomeric tetramer of nonidentical subunits**. *J Biol Chem* 1980, **255**(1):60-65.
15. Said HM: **Cell and molecular aspects of human intestinal biotin absorption**. *J Nutr* 2009, **139**(1):158-162.
16. Wang H, Huang W, Fei YJ, Xia H, Yang-Feng TL, Leibach FH, Devoe LD, Ganapathy V, Prasad PD: **Human placental Na+-dependent multivitamin transporter. Cloning, functional expression, gene structure, and chromosomal localization**. *J Biol Chem* 1999, **274**(21):14875-14883.
17. Daberkow RL, White BR, Cederberg RA, Griffin JB, Zempleni J: **Monocarboxylate transporter 1 mediates biotin uptake in human peripheral blood mononuclear cells**. *J Nutr* 2003, **133**(9):2703-2706.
18. Halestrap AP, Price NT: **The proton-linked monocarboxylate transporter (MCT) family: structure, function and regulation**. *Biochem J* 1999, **343 Pt 2**:281-299.

19. Price NT, Jackson VN, Halestrap AP: **Cloning and sequencing of four new mammalian monocarboxylate transporter (MCT) homologues confirms the existence of a transporter family with an ancient past**. *Biochem J* 1998, **329 (Pt 2)**:321-328.
20. Balamurugan K, Ortiz A, Said HM: **Biotin uptake by human intestinal and liver epithelial cells: role of the SMVT system**. *Am J Physiol Gastrointest Liver Physiol* 2003, **285**(1):G73-77.
21. Davidson AL, Chen J: **ATP-binding cassette transporters in bacteria**. *Annu Rev Biochem* 2004, **73**:241-268.
22. Gottesman MM, Ambudkar SV: **Overview: ABC transporters and human disease**. *J Bioenerg Biomembr* 2001, **33**(6):453-458.
23. Hosie AH, Allaway D, Jones MA, Walshaw DL, Johnston AW, Poole PS: **Solute-binding protein-dependent ABC transporters are responsible for solute efflux in addition to solute uptake**. *Mol Microbiol* 2001, **40**(6):1449-1459.
24. Hollenstein K, Dawson RJ, Locher KP: **Structure and mechanism of ABC transporter proteins**. *Curr Opin Struct Biol* 2007, **17**(4):412-418.
25. Schneider E, Hunke S: **ATP-binding-cassette (ABC) transport systems: functional and structural aspects of the ATP-hydrolyzing subunits/domains**. *FEMS Microbiol Rev* 1998, **22**(1):1-20.
26. Procko E, O'Mara ML, Bennett WF, Tieleman DP, Gaudet R: **The mechanism of ABC transporters: general lessons from structural and functional studies of an antigenic peptide transporter**. *Faseb J* 2009, **23**(5):1287-1302.
27. Aller SG, Yu J, Ward A, Weng Y, Chittaboina S, Zhuo R, Harrell PM, Trinh YT, Zhang Q, Urbatsch IL *et al*: **Structure of P-glycoprotein reveals a molecular basis for poly-specific drug binding**. *Science* 2009, **323**(5922):1718-1722.
28. Rodionov DA, Hebbeln P, Eudes A, ter Beek J, Rodionova IA, Erkens GB, Slotboom DJ, Gelfand MS, Osterman AL, Hanson AD *et al*: **A novel class of modular transporters for vitamins in prokaryotes**. *J Bacteriol* 2009, **191**(1):42-51.
29. Karpowich NK, Wang DN: **Assembly and mechanism of a group II ECF transporter**. *Proc Natl Acad Sci U S A* 2013, **110**(7):2534-2539.
30. Erkens GB, Berntsson RP, Fulyani F, Majsnerowska M, Vujicic-Zagar A, Ter Beek J, Poolman B, Slotboom DJ: **The structural basis of modularity in ECF-type ABC transporters**. *Nat Struct Mol Biol* 2011, **18**(7):755-760.
31. Eitinger T, Rodionov DA, Grote M, Schneider E: **Canonical and ECF-type ATP-binding cassette importers in prokaryotes: diversity in modular organization and cellular functions**. *FEMS Microbiol Rev* 2011, **35**(1):3-67.
32. Hebbeln P, Rodionov DA, Alfandega A, Eitinger T: **Biotin uptake in prokaryotes by solute transporters with an optional ATP-binding cassette-containing module**. *Proc Natl Acad Sci U S A* 2007, **104**(8):2909-2914.
33. Xu K, Zhang M, Zhao Q, Yu F, Guo H, Wang C, He F, Ding J, Zhang P: **Crystal structure of a folate energy-coupling factor transporter from Lactobacillus brevis**. *Nature* 2013, **497**(7448):268-271.
34. Berntsson RP, ter Beek J, Majsnerowska M, Duurkens RH, Puri P, Poolman B, Slotboom DJ: **Structural divergence of paralogous S components from ECF-type ABC transporters**. *Proc Natl Acad Sci U S A* 2012, **109**(35):13990-13995.

35. Zhang P, Wang J, Shi Y: **Structure and mechanism of the S component of a bacterial ECF transporter**. *Nature* 2010, **468**(7324):717-720.
36. Erkens GB, Majsnerowska M, ter Beek J, Slotboom DJ: **Energy coupling factor-type ABC transporters for vitamin uptake in prokaryotes**. *Biochemistry* 2012, **51**(22):4390-4396.
37. Polyak SW, Chapman-Smith A, Mulhern TD, Cronan JE, Jr., Wallace JC: **Mutational analysis of protein substrate presentation in the post-translational attachment of biotin to biotin domains**. *J Biol Chem* 2001, **276**(5):3037-3045.
38. Chapman-Smith A, Cronan JE, Jr.: **In vivo enzymatic protein biotinylation**. *Biomol Eng* 1999, **16**(1-4):119-125.
39. Pendini NR, Yap MY, Polyak SW, Cowieson NP, Abell A, Booker GW, Wallace JC, Wilce JA, Wilce MC: **Structural characterization of Staphylococcus aureus biotin protein ligase and interaction partners: an antibiotic target**. *Protein Sci* 2013, **22**(6):762-773.
40. Soares da Costa TP, Tieu W, Yap MY, Pendini NR, Polyak SW, Sejer Pedersen D, Morona R, Turnidge JD, Wallace JC, Wilce MC *et al*: **Selective inhibition of biotin protein ligase from Staphylococcus aureus**. *J Biol Chem* 2012, **287**(21):17823-17832.
41. Basle A, Rummel G, Storici P, Rosenbusch JP, Schirmer T: **Crystal structure of osmoporin OmpC from E. coli at 2.0 A**. *J Mol Biol* 2006, **362**(5):933-942.
42. James CE, Mahendran KR, Molitor A, Bolla JM, Bessonov AN, Winterhalter M, Pages JM: **How beta-lactam antibiotics enter bacteria: a dialogue with the porins**. *PLoS One* 2009, **4**(5):e5453.
43. Nikaido H: **Molecular basis of bacterial outer membrane permeability revisited**. *Microbiol Mol Biol Rev* 2003, **67**(4):593-656.
44. Jeanteur D, Schirmer T, Fourel D, Simonet V, Rummel G, Widmer C, Rosenbusch JP, Pattus F, Pages JM: **Structural and functional alterations of a colicin-resistant mutant of OmpF porin from Escherichia coli**. *Proc Natl Acad Sci U S A* 1994, **91**(22):10675-10679.
45. Thiolas A, Bornet C, Davin-Regli A, Pages JM, Bollet C: **Resistance to imipenem, cefepime, and cefpirome associated with mutation in Omp36 osmoporin of Enterobacter aerogenes**. *Biochem Biophys Res Commun* 2004, **317**(3):851-856.
46. Iyer R, Delcour AH: **Complex inhibition of OmpF and OmpC bacterial porins by polyamines**. *J Biol Chem* 1997, **272**(30):18595-18601.
47. Fisher DJ, Fernandez RE, Adams NE, Maurelli AT: **Uptake of biotin by Chlamydia Spp. through the use of a bacterial transporter (BioY) and a host-cell transporter (SMVT)**. *PLoS One* 2012, **7**(9):e46052.
48. Drew D, Lerch M, Kunji E, Slotboom DJ, de Gier JW: **Optimization of membrane protein overexpression and purification using GFP fusions**. *Nat Methods* 2006, **3**(4):303-313.
49. Newby ZE, O'Connell JD, 3rd, Gruswitz F, Hays FA, Harries WE, Harwood IM, Ho JD, Lee JK, Savage DF, Miercke LJ *et al*: **A general protocol for the crystallization of membrane proteins for X-ray structural investigation**. *Nat Protoc* 2009, **4**(5):619-637.
50. Wiener MC: **A pedestrian guide to membrane protein crystallization**. *Methods* 2004, **34**(3):364-372.
51. Lin SH, Guidotti G: **Purification of membrane proteins**. *Methods Enzymol* 2009, **463**:619-629.
52. le Maire M, Champeil P, Moller JV: **Interaction of membrane proteins and lipids with**

solubilizing detergents. *Biochim Biophys Acta* 2000, **1508**(1-2):86-111.

53. Arachea BT, Sun Z, Potente N, Malik R, Isailovic D, Viola RE: **Detergent selection for enhanced extraction of membrane proteins**. *Protein Expr Purif*, **86**(1):12-20.

Supplementary Table 1: Results form the filter disc diffusion assay

BioY mutants		Diameter zone of growth inhibition (mm)								
		Erythromycin			Chloramphenicol			Streptomycin		
WT	NI	16	14	15	31	28	33	24	24	26
	0.4%Ara	25	21	20	48	49	49	40	39	37
R75K	NI	18	16	17	30	38	31	25	29	29
	0.4%Ara	25	10	21	46	47	42	37	37	38
K160E	NI	17	16	15	33	33	32	26	28	28
	0.4%Ara	19	11	25	52	49	50	40	41	38
R75C	NI	15	14	16	30	28	32	27	28	26
	0.4%Ara	23	18	21	43	43	47	35	36	36
D128K	NI	15	16	16	28	29	35	24	23	28
	0.4%Ara	23	22	20	43	46	49	37	36	38
D128A	NI	15	13	15	31	30	31	25	26	27
	0.4%Ara	25	23	23	49	48	47	40	40	37
F143A	NI	17	15	15	33	30	32	27	25	27
	0.4%Ara	23	22	26	51	50	49	35	41	39
F143C	NI	18	15	15	34	31	33	27	27	25
	0.4%Ara	23	21	22	48	48	47	38	39	40
V80A/E109D	NI	16	15	14	33	30	29	27	25	26
	0.4%Ara	27	22	21	50	52	52	44	43	43
T54S/F81S	NI	15	13	13	33	30	30	26	N/A	26
	0.4%Ara	24	26	20	52	52	51	43	44	43
N38S	NI	18	15	19	30	32	34	26	25	28
	0.4%Ara	21	21	21	51	50	47	40	40	40
T177S	NI	16	17	16	30	32	34	25	24	29
	0.4%Ara	23	20	22	51	50	46	40	42	38

BioY mutants		Diameter zone of growth inhibition (mm)								
		Erythromycin			Chloramphenicol			Streptomycin		
I139V/A152P	NI	15	13	13	24	27	28	23	25	25
	0.4%Ara	23	21	19	49	48	47	40	39	40
F88V	NI	13	12	14	27	24	28	21	21	19
	0.4%Ara	25	24	30	50	53	52	41	42	42
L68M/F106C	NI	19	18	19	36	35	34	31	29	30
	0.4%Ara	20	22	20	47	45	48	39	38	40
Insert	NI	17	15	14	33	32	30	27	26	28
	0.4%Ara	25	26	23	51	45	45	42	39	40
R75A	NI	16	15	16	34	33	34	29	27	26
	0.4%Ara	26	25	24	50	52	53	41	41	38
D157A	NI	18	16	18	37	31	36	30	29	32
	0.4%Ara	19	27	23	50	46	N/A	38	37	40
D157K/K160E	NI	16	17	16	30	30	33	26	26	27
	0.4%Ara	16	18	16	33	30	32	25	26	25
R75E	NI	N/A	12	12	28	31	33	27	27	27
	0.4%Ara	24	24	20	51	50	53	39	39	39
S85T	NI	14	N/A	16	32	31	32	27	27	27
	0.4%Ara	N/A	22	25	52	49	49	39	40	39
F29A	NI	16	13	16	35	32	30	26	25	26
	0.4%Ara	22	19	25	52	45	51	40	39	39
D157K	NI	16	18	18	36	35	38	31	30	28
	0.4%Ara	27	24	25	49	51	58	40	40	40
K160E	NI	15	15	12	36	34	33	28	29	27
	0.4%Ara	18	22	21	48	49	49	37	38	36

Legend

NI: Samples were not induced;

0.4%Ara: Samples induced with 0.4% arabinose;

N/A: not available